Electronic Supplementary Information

Dinuclear iridium complexes ligated by lithium-ion endohedral fullerene $Li^{+}@C_{60}$

Chinari Fukushi, Takashi Komuro* and Hisako Hashimoto*

Department of Chemistry, Graduate School of Science, Tohoku University, Sendai 980-8578, Japan.

To whom correspondence should be addressed.
hisako.hashimoto.b7@tohoku.ac.jp
takashi.komuro.c5@tohoku.ac.jp

Contents

1. Experimental procedures and characterisation data

General procedures. All manipulations were performed in a glovebox (Ar atmosphere) or using Schlenk techniques (N_2 atmosphere) unless otherwise indicated.

Materials. All solvents were dried and stored under argon over 4 Å molecular sieves in a glovebox prior to use. Et_2O, THF and MeCN were dried using a Glass Contour alumina column (Nikko Hansen & Co., Ltd.). CD_2Cl_2, $CHCl_3$, $CDCl_3$, TCE (1,1,2,2-tetrachloroethane) and *o*-DCB (1,2-dichlorobenzene) were dried over CaH_2 and distilled before use. $Ir_2X_2(cod)_2$ (X = Cl[S1] and I[S2]) were prepared according to the literature procedures. $Ir_2Br_2(cod)_2$ was synthesised with some modification of the literature procedure[S2] (see below). $[Li^+@C_{60}](NTf_2^-)$ was prepared by the anion exchange of $[Li^+@C_{60}](PF_6^-)$, which was supplied from Idea International Corporation, with $LiNTf_2$.[S3] LiBr was purchased from Tokyo Chemical Industry Co., Ltd. $AgNO_3$ was purchased from Kanto Chemical Co., Inc. $[^nBu_4N](PF_6^-)$ was purchased from FUJIFILM Wako Pure Chemical Co., Ltd. and recrystallized from hot EtOH prior to use. $[^nBu_4N](NTf_2^-)$ was prepared by the anion exchange of $[^nBu_4N](Cl^-)$, which was purchased from Kanto Chemical Co., Ltd., with $LiNTf_2$.

Spectroscopic measurements. The NMR spectra were recorded on a Bruker AVANCE III 400 Fourier transform spectrometer (^{1}H: 400.1 MHz, ^{7}Li: 155.5 MHz, ^{13}C: 100.6 MHz). Chemical shifts are reported in parts per million. Line widths at half-height ($\Delta\nu_{1/2}$) are given in Hz. ^{1}H NMR chemical shifts were referenced to the residual proton ($CHCl_3$: 7.26 ppm and $CDHCl_2$: 5.32 ppm). ^{7}Li NMR chemical shifts were referenced to LiCl/D_2O (0.0 ppm) as an external standard. $^{13}C\{^1H\}$ NMR chemical shifts were referenced to the carbon of deuterated solvents ($CDCl_3$: 77.2 ppm and CD_2Cl_2: 53.8 ppm). $^{13}C\{^1H\}$ NMR signals of cod ligands were assigned based on ^1H–^{13}C HSQC experiments. All NMR data were collected at room temperature unless otherwise indicated. High-resolution mass spectra (HRMS) were obtained by use of a Bruker Daltonics solariX 9.4T spectrometer operating in the electrospray ionisation (ESI) mode. Elemental analysis was performed using a J-Science Lab JM11 microanalyzer. Measurements of HRMS and elemental analysis were performed at the Research and Analytical Center for Giant Molecules, Tohoku University. UV/Vis spectra were measured on a Shimadzu Multi-Spec-1500 spectrometer. Cyclic Voltammetry (CV) and Differential Pulse Voltammetry (DPV) measurements were performed using a BAS ALS-620D electrochemical analyser.

1-1. Modified procedure for the synthesis of $Ir_2Br_2(cod)_2$

$Ir_2Cl_2(cod)_2$ (152 mg, 226 mmol) and LiBr (153 mg, 1.77 mmol, 7.8 equiv.) were placed in a 50 mL Schlenk flask, which was moved into a glove box. THF (5 mL) and $CHCl_3$ (5 mL) were added to the reactants to give a yellow solution. After the solution was stirred at room temperature for 20 h, the colour of the solution turned into orange. The solution was then evapourated under vacuum. The resulting reddish orange solid was extracted with *ca.* 10 mL of $CHCl_3$ and filtered. The filtrate was evapourated under vacuum to dryness, which afforded a dark red solid of $Ir_2Br_2(cod)_2$ (171 mg, 225 mmol, 99%). $Ir_2Br_2(cod)_2$ was identified by comparison of the ^{1}H NMR data with the literature values,[S2] and its purity was confirmed by the elemental analysis. ^{1}H NMR ($CDCl_3$): δ 4.30–4.38 (br m, 8H, CH), 2.13–2.29 (br m, 8H, CH_2), 1.37–1.52 (br m, 8H, CH_2); $^{13}C\{^1H\}$ NMR ($CDCl_3$): δ 62.4 (s, CH), 32.0 (s, CH_2); Anal. calcd. for $C_{16}H_{24}Br_2Ir_2$: C, 25.27; H, 3.18; found: C, 25.33; H, 3.29; UV/Vis (CH_2Cl_2, 1.0×10^{-3} M, 1 mm quartz cell) λ_{max} / nm (ε / M^{-1} cm^{-1}): 334 (2.4×10^3), 405 (2.4×10^3), 473 (4.2×10^3), 673 (63).

1-2. Synthesis of $[\{\mu\text{-}\eta^2\text{:}\eta^2\text{-}(Li^+@C_{60})\}\{Ir_2Cl_2(cod)_2\}](NTf_2^-)$ (1)

In the air, $[Li^+@C_{60}](NTf_2^-)$ (1.22 mg, 1.21 μmol) was weighed into a 5 mL vial equipped with a magnetic stirring bar, and $Ir_2Cl_2(cod)_2$ (0.81 mg, 1.21 μmol, 1.0 equiv.) was weighed into another 5 mL vial. These vials were moved into a glove box. To each of the vials, 1,1,2,2-tetrachloroethane (TCE) (0.2 and 0.4 mL, respectively) was added and mixed. The resulting yellow solution of $Ir_2Cl_2(cod)_2$ was added to the purple solution of $[Li^+@C_{60}](NTf_2^-)$ with stirring. The colour of the solution instantaneously turned into dark reddish-brown. After stirring at room temperature for 5 min, the reaction mixture was filtered. Recrystallisation from the filtrate by vapour diffusion of Et_2O as poor solvent at −30 °C afforded complex **1** as black crystals (1.80 mg, 1.07 μmol, 89%). ^{1}H NMR (CD_2Cl_2): δ 5.33–5.45 (br m, 2H, CH), 4.92–5.15 (br m, 4H, CH), 3.62–3.83 (br m, 2H, CH), 2.78–3.00 (br m, 2H, CH_2), 2.61–2.74 (br m, 2H, CH_2), 2.48–2.61 (br m, 2H, CH_2), 2.33–2.48 (br m, 4H, CH_2), 2.01–2.33 (br m, 4H, CH_2), 1.66–1.76 (br m, 2H, CH_2); ^{7}Li NMR (CD_2Cl_2): δ −11.0 (br s, $\Delta\nu_{1/2}$ = 14 Hz); HRMS (ESI, positive) *m*/*z* calcd. for $[^{12}C_{76}{}^1H_{24}{}^7Li^{35}Cl_2{}^{193}Ir_2]^+$ ($[M]^+$): 1399.0667, found: 1399.0682; UV/Vis (CH_2Cl_2, 1.0×10^{-4} M, 1 mm quartz cell) λ_{max} / nm (ε / M^{-1} cm^{-1}): 327 (4.4×10^4), 416 (9.8×10^3), 530 (3.5×10^3).

1-3. Synthesis of [{μ-η^2:η^2-(Li$^+$@C$_{60}$)}{Ir$_2$Br$_2$(cod)$_2$}](NTf$_2^-$) (2)

In a procedure similar to that for complex **1**, the title compound was synthesised using [Li$^+$@C$_{60}$](NTf$_2^-$) (1.42 mg, 1.41 μmol) and Ir$_2$Br$_2$(cod)$_2$ (1.07 mg, 1.41 μmol, 1.0 equiv.) in TCE. Filtration of the resulting dark reddish-brown reaction mixture, followed by recrystallisation and vapour diffusion of Et$_2$O at −30 °C afforded complex **2** as black crystals (2.14 mg, 1.21 μmol, 86%). ^{1}H NMR (CD$_2$Cl$_2$): δ 5.16–5.30 (br m, 4H, CH), 5.04–5.16 (br m, 2H, CH), 3.57–3.84 (br m, 2H, CH), 2.86–3.07 (br m, 2H, CH$_2$), 2.67–2.86 (br m, 2H, CH$_2$), 2.42–2.67 (br m, 4H, CH$_2$), 2.26–2.42 (br m, 4H, CH$_2$), 2.11–2.26 (br m, 2H, CH$_2$), 1.45–1.65 (br m, 2H, CH$_2$); ^{7}Li NMR (CD$_2$Cl$_2$): δ −11.0 (br s, $\Delta\nu_{1/2}$ = 26 Hz); HRMS (ESI, positive) *m*/*z* calcd. for [^{12}C$_{76}$^{1}H$_{24}$^{7}Li^{79}Br$_2$^{193}Ir$_2$]$^+$ ([M]$^+$): 1488.9642, found: 1488.9639; UV/Vis (CH$_2$Cl$_2$, 1.0 × 10^{-4} M, 1 mm quartz cell) λ_{max} / nm (ε / M^{-1} cm^{-1}): 327 (4.2 × 10^4), 420 (1.2 × 10^4), 538 (5.1 × 10^3).

1-4. Synthesis of [{μ-η^2:η^2-(Li$^+$@C$_{60}$)}{Ir$_2$I$_2$(cod)$_2$}](NTf$_2^-$) (3)

In a procedure similar to that for complex **1**, the title compound was synthesised using [Li$^+$@C$_{60}$](NTf$_2^-$) (2.00 mg, 1.98 μmol) and Ir$_2$I$_2$(cod)$_2$ (1.71 mg, 2.00 μmol , 1.0 equiv.) in TCE. The dark reddish-brown reaction mixture was worked up similarly to give complex **3** as black crystals (3.34 mg, 1.79 μmol, 90%). ^{1}H NMR (CD$_2$Cl$_2$): δ 5.30–5.60 (br m, 2H, CH), 5.20–5.30 (br m, 2H, CH), 4.96–5.20 (br m, 2H, CH), 3.39–3.80 (br m, 2H, CH), 2.75–3.27 (br m, 4H, CH$_2$), 2.36–2.75 (br m, 6H, CH$_2$), 2.15–2.36 (br m, 2H, CH$_2$), 1.84–2.15 (br m, 2H, CH$_2$), 1.18–1.63 (br m, 2H, CH$_2$); ^{7}Li NMR (CD$_2$Cl$_2$): δ −11.0 (br s, $\Delta\nu_{1/2}$ = 32 Hz); HRMS (ESI, positive) *m*/*z* calcd. for [^{12}C$_{76}$^{1}H$_{25}$^{16}O^{7}Li^{127}I^{193}Ir$_2$]$^+$ ([M – ^{127}I + ^{1}H + ^{16}O]$^+$): 1473.0377, found: 1473.0373; *m*/*z* calcd. for [^{12}C$_{76}$^{1}H$_{24}$^{7}Li^{35}Cl^{127}I^{193}Ir$_2$]$^+$ ([M – ^{127}I + ^{35}Cl]$^+$): 1491.0033, found: 1491.0024;* UV/Vis (CH$_2$Cl$_2$, 1.0 × 10^{-4} M, 1 mm quartz cell) λ_{max} / nm (ε / M^{-1} cm^{-1}): 328 (5.1 × 10^4), 415 (1.5 × 10^4), 550 (6.9 × 10^3).

*Note: In the mass spectrum of complex **3**, the molecular ion peak of the cation part of **3** was not detected. Instead, the peaks of cations, in which one iodido ligand was replaced with OH or Cl, were observed (Figs. S30 and S31), possibly as a result of facile hydrolysis with H$_2$O or the reaction with CHCl$_3$ used as a washing solvent during the measurement. These data support the core structure of **3** and thus are indicated here.

1-5. Measurements of VT $^{13}C\{^1H\}$ and low temperature 2D NMR spectra of 1

In a glove box, complex **1** (5.23 mg, 3.11 μmol) was placed in a Pyrex NMR tube (5 mm o.d.) fitted with a ground-glass joint, and then CD_2Cl_2 (0.4 mL) was added and mixed to form a dark reddish-brown solution. The NMR tube was equipped with a Teflon valve and connected to a vacuum line. After the solution was degassed by a freeze-pump-thaw cycle, the NMR tube was sealed under reduced pressure using a gas burner. The $^{13}C\{^1H\}$ NMR spectra of the sample were collected at 300 and 200 K. The ^1H–^1H COSY and ^1H–^{13}C HSQC spectra were measured at 200 K.

$^{13}C\{^1H\}$ NMR (CD_2Cl_2, 300 K): δ 140–150 (br m, C_{60}), 120.3 (q, $^1J_{CF}$ = 319.2 Hz, CF_3 of NTf_2^-), 90.5 (s, CH of cod), 89.3 (s, CH of cod), 80.0 (s, CH of cod), 75.3 (s, CH of cod), 39.9 (s, CH_2 of cod), 37.8 (s, CH_2 of cod), 28.1 (s, CH_2 of cod), 25.4 (s, CH_2 of cod).

$^{13}C\{^1H\}$ NMR (CD_2Cl_2, 200 K): δ 152.0 (s, C_{60}), 149.0 (s, C_{60}), 148.1 (s, C_{60}), 146.4 (s, C_{60}), 145.5 (s, C_{60}), 145.4 (s, C_{60}), 145.1 (s, C_{60}), 145.0 (s, C_{60}), 144.7 (s, C_{60}), 144.5 (s, C_{60}), 144.22 (s, C_{60}), 144.17 (s, C_{60}), 144.0 (s, C_{60}), 143.7 (s, C_{60}), 143.4 (s, C_{60}), 143.3 (s, C_{60}), 143.2 (s, C_{60}), 142.7 (s, C_{60}), 142.6 (s, C_{60}), 142.4 (s, C_{60}), 142.2 (s, C_{60}), 141.3 (s, C_{60}), 141.0 (s, C_{60}), 140.9 (s, C_{60}), 140.4 (s, C_{60}), 139.7 (s, C_{60}), 137.2 (s, C_{60}), 135.5 (s, C_{60}), 118.9 (q, $^1J_{CF}$ = 318.5 Hz, CF_3 of NTf_2^-), 89.9 (s, CH of cod), 88.7 (s, CH of cod), 83.3 (s, Ir−C of C_{60}), 78.6 (s, CH of cod), 74.3 (s, CH of cod), 57.5 (s, Ir−C of C_{60}), 39.2 (s, CH_2 of cod), 37.1 (s, CH_2 of cod), 26.8 (s, CH_2 of cod), 24.3 (s, CH_2 of cod).

2. X-ray crystal structure analysis

General procedures. Single crystals of **1·$C_2H_2Cl_4$**, **2·$C_2H_2Cl_4$** and **3·$C_2H_2Cl_4$** suitable for X-ray diffraction were obtained by vapour diffusion of Et_2O into a TCE solution of complexes **1**–**3** at −30 °C in a week. X-ray diffraction data were collected on a Rigaku XtaLAB mini II diffractometer with graphite-monochromated Mo Kα radiation (λ = 0.71073 Å) under cold nitrogen stream (T = 150 K). Single crystals suitable for diffraction measurements were coated with liquid paraffin and were mounted on a polyimide loop. Empirical absorption correction using the multiscan method was applied to the data. The structures were solved by dual space methods using SHELXT[S4] and refined by full-matrix least-squares technique on F^2 with SHELXL[S5] using Olex2 1.5 software[S6] (OlexSys Ltd, 2018) or Yadokari-XG 2009 software[S7,S8] as graphical user interfaces. Except disordered atoms described below, all hydrogen atoms were placed at their geometrically calculated positions and refined riding on the corresponding carbon atoms with isotropic thermal parameters. All non-hydrogen atoms were refined anisotropically. CCDC reference numbers: 2389980 (for **1·$C_2H_2Cl_4$**), 2389981 (for **2·$C_2H_2Cl_4$**) and 2389982 (for **3·$C_2H_2Cl_4$**). Crystallographic data are available as a CIF file.

2-1. Refinement details on the crystal structure analysis

1·$C_2H_2Cl_4$: The crystal contains three kinds of disordered moieties, i.e., the Li^+ centre, the counter anion (NTf_2^-) and the crystal solvent ($C_2H_2Cl_4$). The lithium atom was disordered in two positions (53% and 47% occupancy) and was refined with anisotropic temperature factors suppressed using SIMU and ISOR commands of the SHELXL program. All atoms of the counter anion (NTf_2^-) were disordered in three positions (41%, 38% and 21% occupancy).[*1] The crystal solvent ($C_2H_2Cl_4$) was also disordered in three positions (44%, 30% and 26% occupancy).[*1] For the disordered NTf_2^- and $C_2H_2Cl_4$, their geometrical positions were suppressed using DFIX and DANG commands and refined anisotropically. The temperature factors of these atoms were treated with the RIGU and SIMU commands or constrained using the EADP command. In some cases, the ISOR command was also used for restraint of the temperature factors. The final R-factors were $R1$ = 0.0274 and $wR2$ = 0.0655 for 12686 reflections with $I > 2\sigma(I)$.

[Note *1] We also examined the analysis using a two-component model, but the three-component model gave us better results that were reported here.

2·$C_2H_2Cl_4$: The crystal contains three kinds of disordered moieties, i.e., the Li^+ centre, the counter anion (NTf_2^-) and crystal solvent ($C_2H_2Cl_4$). The lithium atom was disordered in two positions (60% and 40% occupancy) and was refined with anisotropic temperature factors suppressed using SIMU and ISOR commands of the SHELXL program. All atoms of the counter anion (NTf_2^-) were disordered in three positions (45%, 29% and 26% occupancy).[*1] The crystal solvent ($C_2H_2Cl_4$) was also disordered in three positions (53%, 28% and 19% occupancy).[*1] For the disordered NTf_2^- and $C_2H_2Cl_4$, their geometrical positions were suppressed using DFIX and DANG commands and refined anisotropically. The temperature factors of these atoms were treated with the RIGU and SIMU commands or constrained using the EADP command. In some cases, the ISOR command was also used for restraint of the temperature factors. The final *R*-factors were $R1 = 0.0323$ and $wR2 = 0.0713$ for 12758 reflections with $I > 2\sigma(I)$.

[Note *1] We also examined the analysis using a two-component model, but the three-component model gave us better results that were reported here.

3·$C_2H_2Cl_4$: The crystal contains three kinds of disordered moieties, i.e., the Li^+ centre, the counter anion (NTf_2^-) and crystal solvent ($C_2H_2Cl_4$). The lithium atom was disordered in two positions (60% and 40% occupancy) and was refined with anisotropic temperature factors suppressed using SIMU and ISOR commands of the SHELXL program. All atoms of the counter anion (NTf_2^-) were also disordered in two positions (68% and 32% occupancy).[*2] The crystal solvent ($C_2H_2Cl_4$) was disordered in two positions (68% and 32% occupancy).[*2] For the disordered NTf_2^- and $C_2H_2Cl_4$, their geometrical positions were suppressed using DFIX and DANG commands and refined anisotropically. The temperature factors of these atoms were treated with the RIGU and SIMU commands or constrained using the EADP command. In some cases, the ISOR command was also used for restraint of the temperature factors. The final *R*-factors were $R1 = 0.0432$ and $wR2 = 0.1148$ for 10156 reflections with $I > 2\sigma(I)$.[*3]

[Note *2] For **3·$C_2H_2Cl_4$**, the analysis of the disordering moieties (the counter anion and crystal solvents) using a three-component model did not give better results than that using the two-component model, which was reported here.

[Note *3] In the checkCIF report, the following level A alerts remain.

PLAT972_ALERT_2_A Check Calcd Resid. Dens. 0.79Ang From I1 −3.85 e A^{-3}
PLAT972_ALERT_2_A Check Calcd Resid. Dens. 0.76Ang From I1 −3.57 e A^{-3}

We tried to improve them using numerical and empirical absorption correction methods and also re-analysis by omitting very weak reflections, but all these efforts resulted in failure. Nevertheless, we believe that the core structure of **3** is confirmed by the present analysis.

Table S1 Crystallographic data

Compound	**1·$C_2H_2Cl_4$**	**2·$C_2H_2Cl_4$**	**3·$C_2H_2Cl_4$**
Empirical formula	$C_{80}H_{26}LiNO_4F_6S_2Cl_6Ir_2$	$C_{80}H_{26}LiNO_4F_6S_2Cl_4Br_2Ir_2$	$C_{80}H_{26}LiNO_4F_6S_2Cl_4I_2Ir_2$
Formula weight	1847.18	1936.10	2030.08
Temperature / K	150(2)	150(2)	150(2)
Crystal system	Triclinic	Triclinic	Triclinic
Space group	$P-1$ (#2)	$P-1$ (#2)	$P-1$ (#2)
a / Å	13.6564(2)	13.6166(2)	13.6521(3)
b / Å	14.5752(4)	14.6678(3)	14.7289(3)
c / Å	15.8044(4)	15.8666(3)	16.0559(3)
α / °	115.334(3)	115.5674(19)	115.704(2)
β / °	98.0777(16)	97.7068(14)	97.1726(18)
γ / °	92.7062(16)	93.1991(13)	93.7882(18)
V / Å^3	2794.71(13)	2809.83(10)	2860.07(11)
Z	2	2	2
ρ_{calcd} / g·cm^{-3}	2.195	2.288	2.357
μ / mm^{-1}	5.205	6.504	6.072
F(000)	1780	1852	1924
Crystal size / mm^3	0.25 × 0.13 × 0.10	0.14 × 0.13 × 0.05	0.15 × 0.12 × 0.05
2θ range / °	4.080 to 54.966	4.060 to 54.968	4.316 to 50.246
Reflections collected	50708	53901	38933
Independent reflections	12686	12758	10156
R_{int}	0.0245	0.0380	0.0397
Refined parameters	1163	1127	1023
$R1$, $wR2$ [all data]^{a,b}	0.0349, 0.0684	0.0484, 0.0761	0.0537, 0.1209
$R1$, $wR2$ [$I > 2\sigma(I)$]^{a,b}	0.0274, 0.0655	0.0323, 0.0713	0.0432, 0.1148
GOF	1.031	1.025	1.035
Largest residual peak, hole / e·Å^{-3}	3.04 / −1.62	1.39 / −0.76	2.45 / −3.93

$^a R1 = \Sigma \, ||F_o| - |F_c|| \, / \, \Sigma \, |F_o|$, $^b wR2 = \{\Sigma \, [w(F_o^2 - F_c^2)^2] \, / \, \Sigma \, [w(F_o^2)^2]\}^{1/2}$

2-2. Crystal structures and selected bond distances and angles

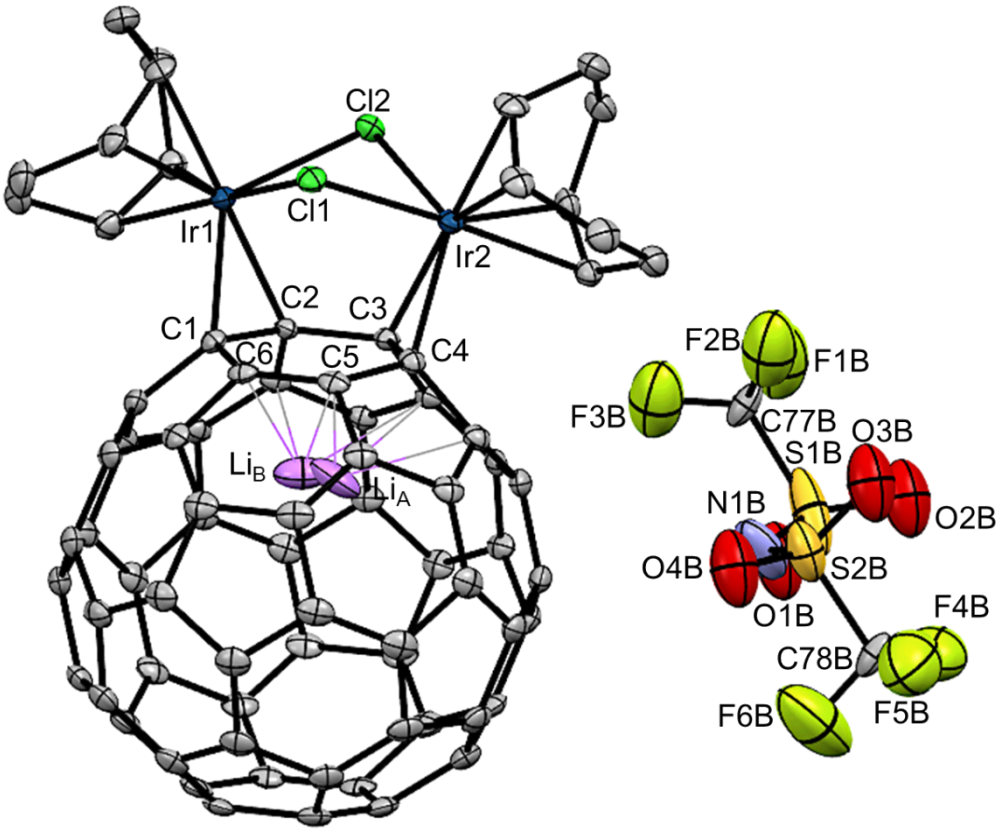

Fig. S1 Molecular structure of **1** with thermal ellipsoids at the 50% probability level. The crystalline solvent $C_2H_2Cl_4$ is omitted. For the disordered counter anion NTf_2^-, only one fragment with the higher occupancy (41%) is shown for clarity. Selected interatomic distances (Å) and angles (°): Ir1–C1 2.170(4), Ir1–C2 2.162(4), Ir2–C3 2.169(4), Ir2–C4 2.170(4), Ir1–Cl1 2.4025(9), Ir1–Cl2 2.5395(9), Ir2–Cl1 2.3955(9), Ir2–Cl2 2.5471(10), C1–C2 1.488(5), C2–C3 1.531(5), C3–C4 1.499(5), C4–C5 1.497(5), C5–C6 1.385(5), C6–C1 1.499(5), Li_A–C1 2.69(7), Li_B–C1 2.34(4), Li_A–C2 2.46(6), Li_B–C2 2.22(4), Li_A–C3 2.22(3), Li_B–C3 2.33(6), Li_A–C4 2.25(3), Li_B–C4 2.56(7), Li_A–C5 2.34(3), Li_B–C5 2.50(5), Li_A–C6 2.55(5), Li_B–C6 2.40(4), Ir1–Cl1–Ir2 92.12(3), Ir1–Cl2–Ir2 85.56(3), Cl1–Ir1–Cl2 78.30(3), Cl1–Ir2–Cl2 78.27(3).

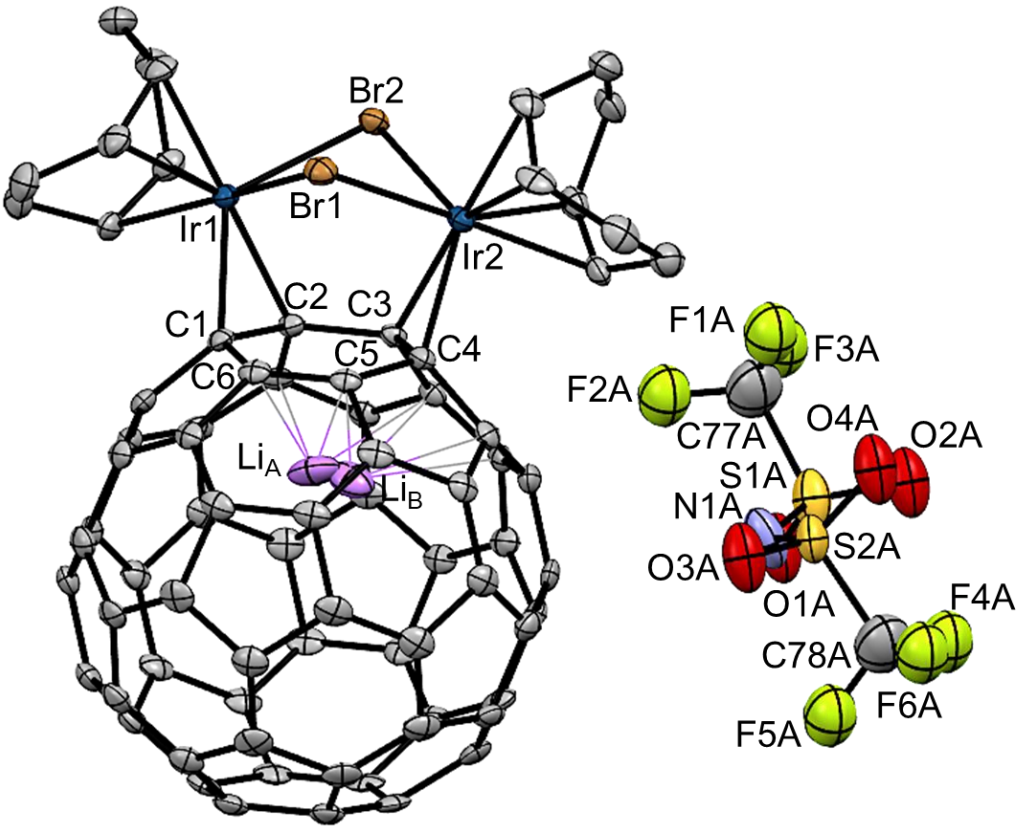

Fig. S2 Molecular structure of **2** with thermal ellipsoids at the 50% probability level. The crystalline solvent $C_2H_2Cl_4$ is omitted. For the disordered counter anion NTf_2^-, only one fragment with the higher occupancy (45%) is shown for clarity. Selected interatomic distances (Å) and angles (°): Ir1–C1 2.177(4), Ir1–C2 2.164(4), Ir2–C3 2.166(4), Ir2–C4 2.169(4), Ir1–Br1 2.5269(5), Ir1–Br2 2.6428(5), Ir2–Br1 2.5255(5), Ir2–Br2 2.6489(5), C1–C2 1.494(6), C2–C3 1.542(6), C3–C4 1.489(6), C4–C5 1.510(6), C5–C6 1.372(7), C6–C1 1.502(7), Li_A–C1 2.38(4), Li_B–C1 2.81(9), Li_A–C2 2.26(3), Li_B–C2 2.52(8), Li_A–C3 2.32(4), Li_B–C3 2.23(5), Li_A–C4 2.51(5), Li_B–C4 2.28(5), Li_A–C5 2.45(4), Li_B–C5 2.45(5), Li_A–C6 2.40(3), Li_B–C6 2.68(8), Ir1–Br1–Ir2 89.012(17), Ir1–Br2–Ir2 84.023(15), Br1–Ir1–Br2 79.330(16), Br1–Ir2–Br2 79.237(17).

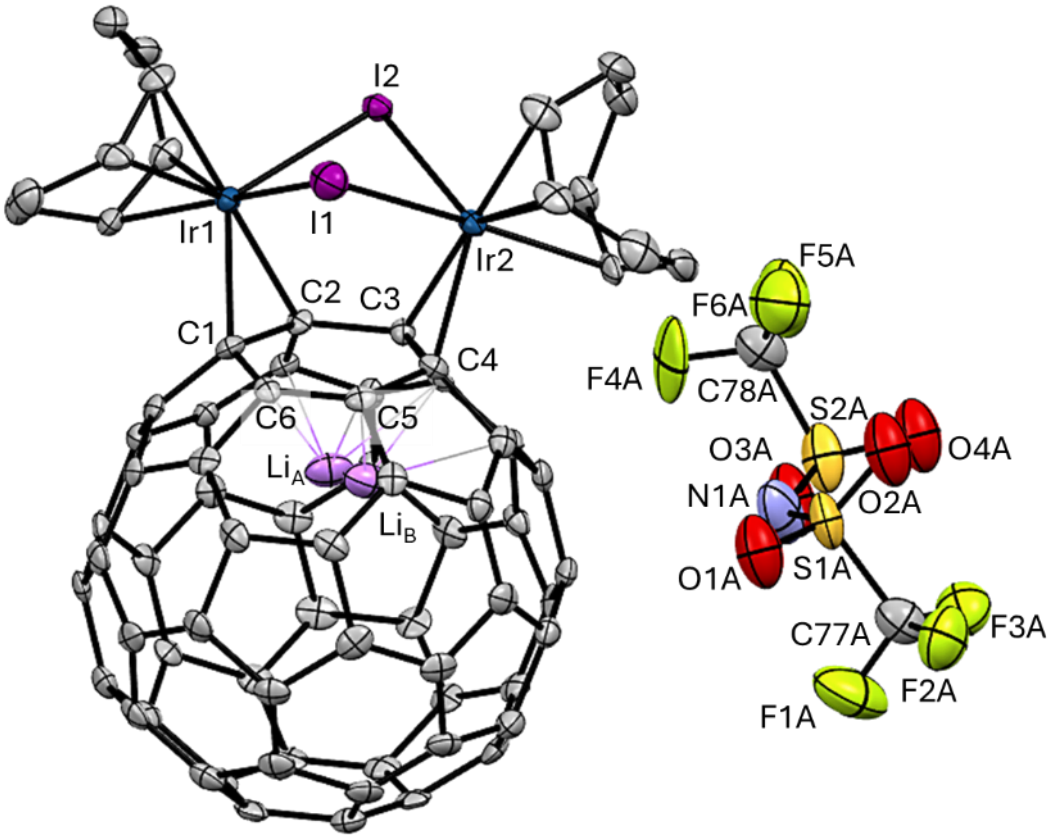

Fig. S3 Molecular structure of **3** with thermal ellipsoids at the 50% probability level. The crystalline solvent $C_2H_2Cl_4$ is omitted for clarity. For the disordered counter anion NTf_2^-, only one fragment with the higher occupancy (68%) is shown for clarity. Selected interatomic distances (Å) and angles (°): Ir1–C1 2.187(8), Ir1–C2 2.184(8), Ir2–C3 2.175(8), Ir2–C4 2.185(8), Ir1–I1 2.6877(8), Ir1–I2 2.7611(6), Ir2–I1 2.6747(7), Ir2–I2 2.7740(6), C1–C2 1.497(11), C2–C3 1.535(11), C3–C4 1.502(11), C4–C5 1.501(11), C5–C6 1.387(11), C6–C1 1.506(11), Li_A–C1 2.38(5), Li_B–C1 2.81(9), Li_A–C2 2.24(5), Li_B–C2 2.57(8), Li_A–C3 2.29(5), Li_B–C3 2.25(7), Li_A–C4 2.47(6), Li_B–C4 2.20(7), Li_A–C5 2.45(5), Li_B–C5 2.32(8), Li_A–C6 2.40(4), Li_B–C6 2.60(9), Ir1–I1–Ir2 85.68(2), Ir1–I2–Ir2 82.402(17), I1–Ir1–I2 80.27(2), I1–Ir2–I2 80.26(2).

Table S2 Selected bond distances (Å) and angles (°) for **1**–**3**

	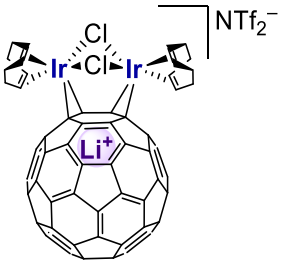	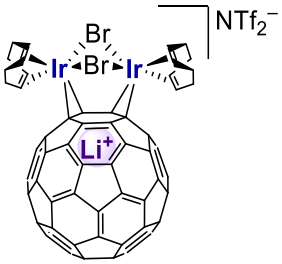	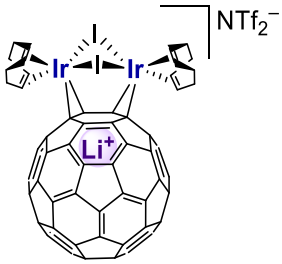
	1	**2**	**3**
Ir1–C1	2.170(4)	2.177(4)	2.187(8)
Ir1–C2	2.162(4)	2.164(4)	2.184(8)
Ir2–C3	2.169(4)	2.166(4)	2.175(8)
Ir2–C4	2.170(4)	2.169(4)	2.185(8)
Ir1–X1	2.4025(9)	2.5269(5)	2.6877(8)
Ir1–X2	2.5395(9)	2.6428(5)	2.7611(6)
Ir2–X1	2.3955(9)	2.5255(5)	2.6747(7)
Ir2–X2	2.5471(10)	2.6489(5)	2.7740(6)
C1–C2	1.488(5)	1.494(6)	1.497(11)
C2–C3	1.531(5)	1.542(6)	1.535(11)
C3–C4	1.499(5)	1.489(6)	1.502(11)
C4–C5	1.497(5)	1.510(6)	1.501(11)
C5–C6	1.385(5)	1.372(7)	1.387(11)
C6–C1	1.499(5)	1.502(7)	1.506(11)
Li_A/Li_B–C1	2.69(7)/2.34(4)	2.38(4)/2.81(9)	2.38(5)/2.81(9)
Li_A/Li_B–C2	2.46(6)/2.22(4)	2.26(3)/2.52(8)	2.24(5)/2.57(8)
Li_A/Li_B–C3	2.22(3)/2.33(6)	2.32(4)/2.23(5)	2.29(5)/2.25(7)
Li_A/Li_B–C4	2.25(3)/2.56(7)	2.51(5)/2.28(5)	2.47(6)/2.20(7)
Li_A/Li_B–C5	2.34(3)/2.50(5)	2.45(4)/2.45(5)	2.45(5)/2.32(8)
Li_A/Li_B–C6	2.55(5)/2.40(4)	2.40(3)/2.68(8)	2.40(4)/2.60(9)
Ir1–X1–Ir2	92.12(3)	89.012(17)	85.68(2)
Ir1–X2–Ir2	85.56(3)	84.023(15)	82.402(17)
X1–Ir1–X2	78.30(3)	79.330(16)	80.27(2)
X1–Ir2–X2	78.27(3)	79.237(17)	80.26(2)

3. NMR spectra and high-resolution mass spectrometry

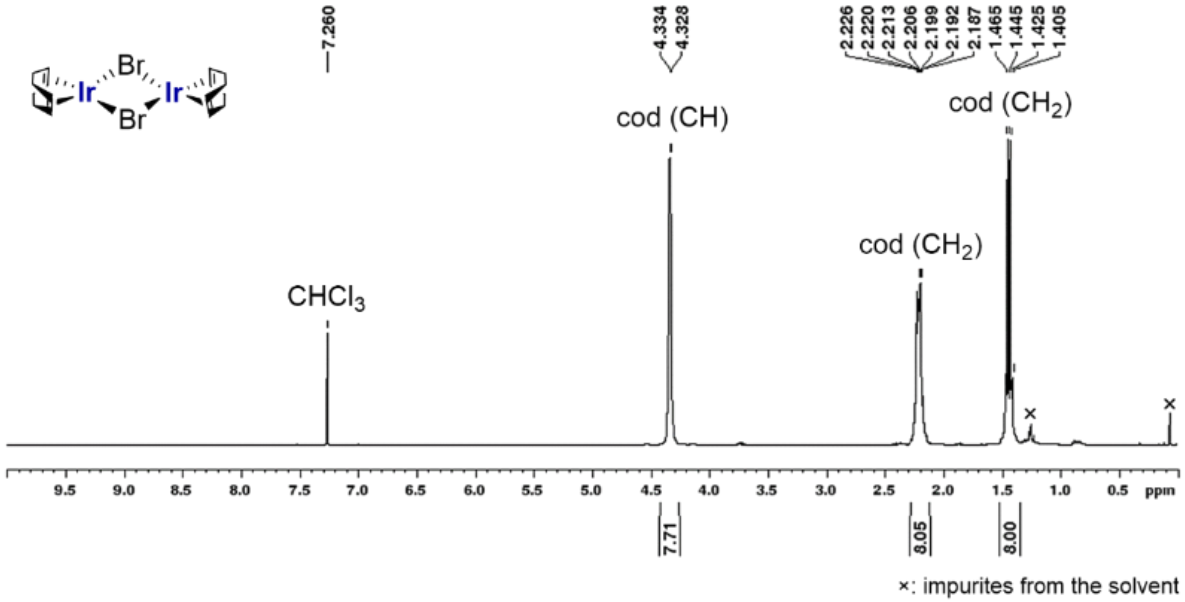

Fig. S4 ^{1}H NMR spectrum of $Ir_2Br_2(cod)_2$ ($CDCl_3$, 400 MHz, r.t.).

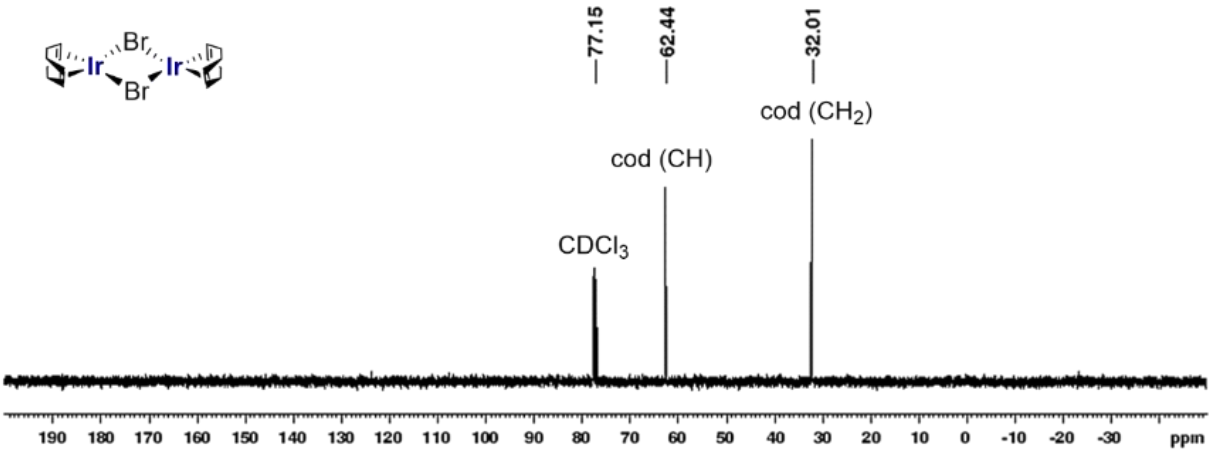

Fig. S5 $^{13}C\{^{1}H\}$ NMR spectrum of $Ir_2Br_2(cod)_2$ ($CDCl_3$, 101 MHz, r.t.).

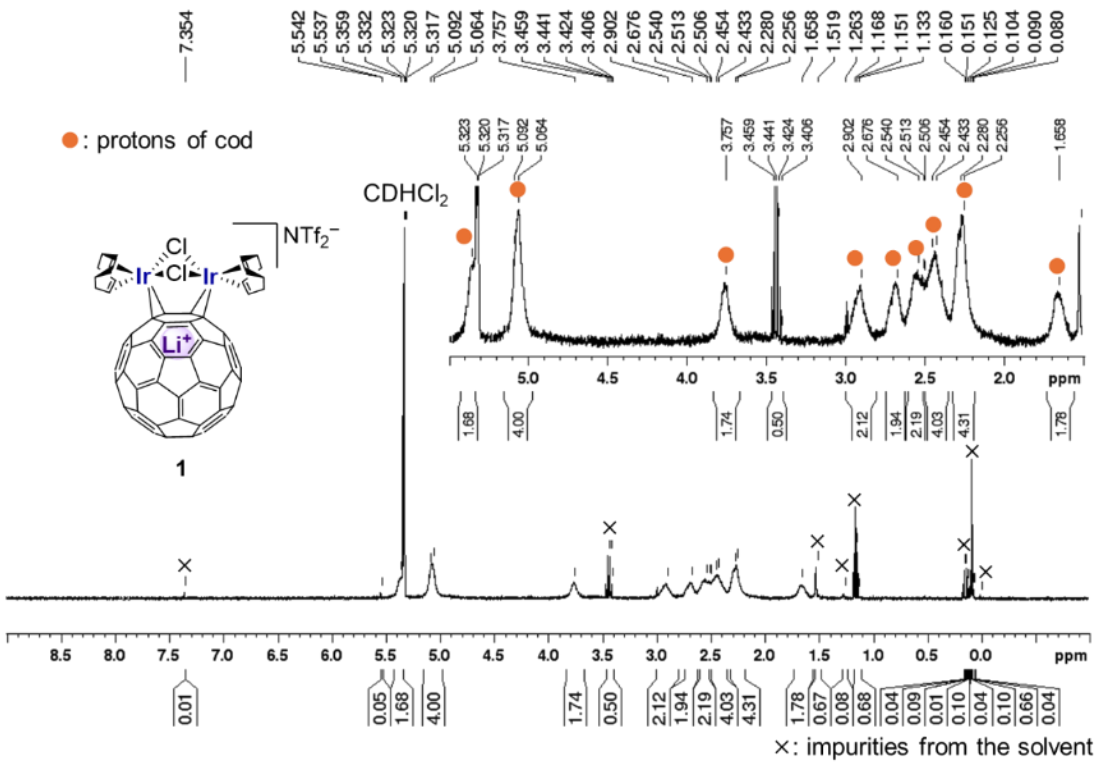

Fig. S6 ^{1}H NMR spectrum of [{μ-η^{2}:η^{2}-(Li^{+}@C$_{60}$)}{Ir$_2$Cl$_2$(cod)$_2$}] (**1**) (CD$_2$Cl$_2$, 400 MHz, r.t.).

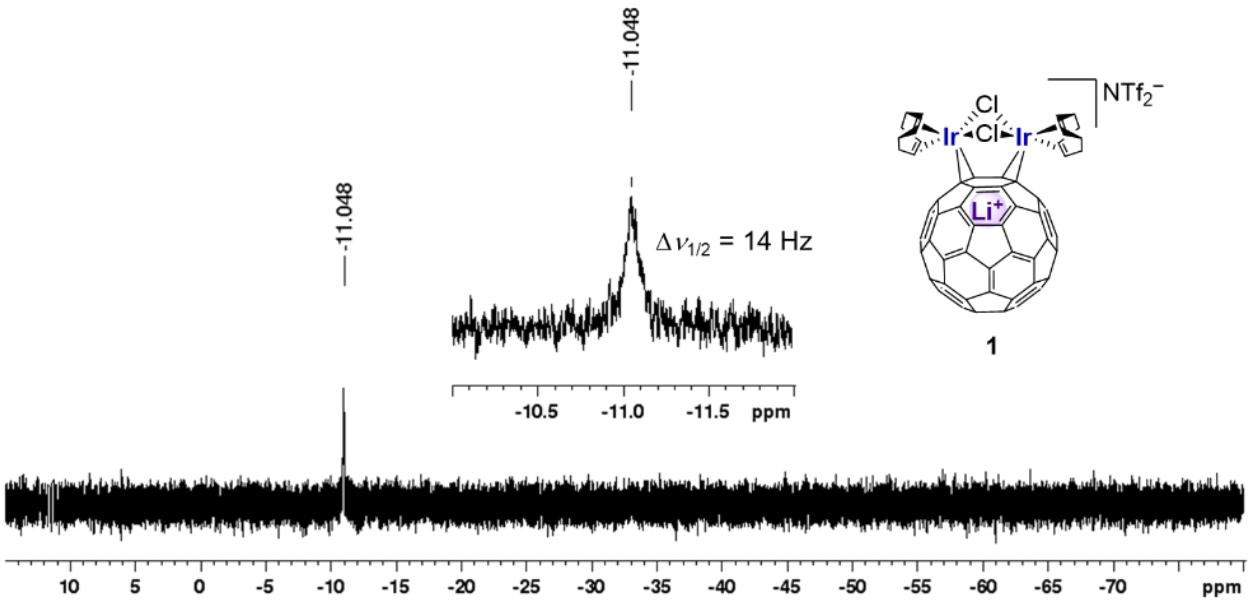

Fig. S7 ^{7}Li NMR spectrum of **1** (CD$_2$Cl$_2$, 156 MHz, r.t.).

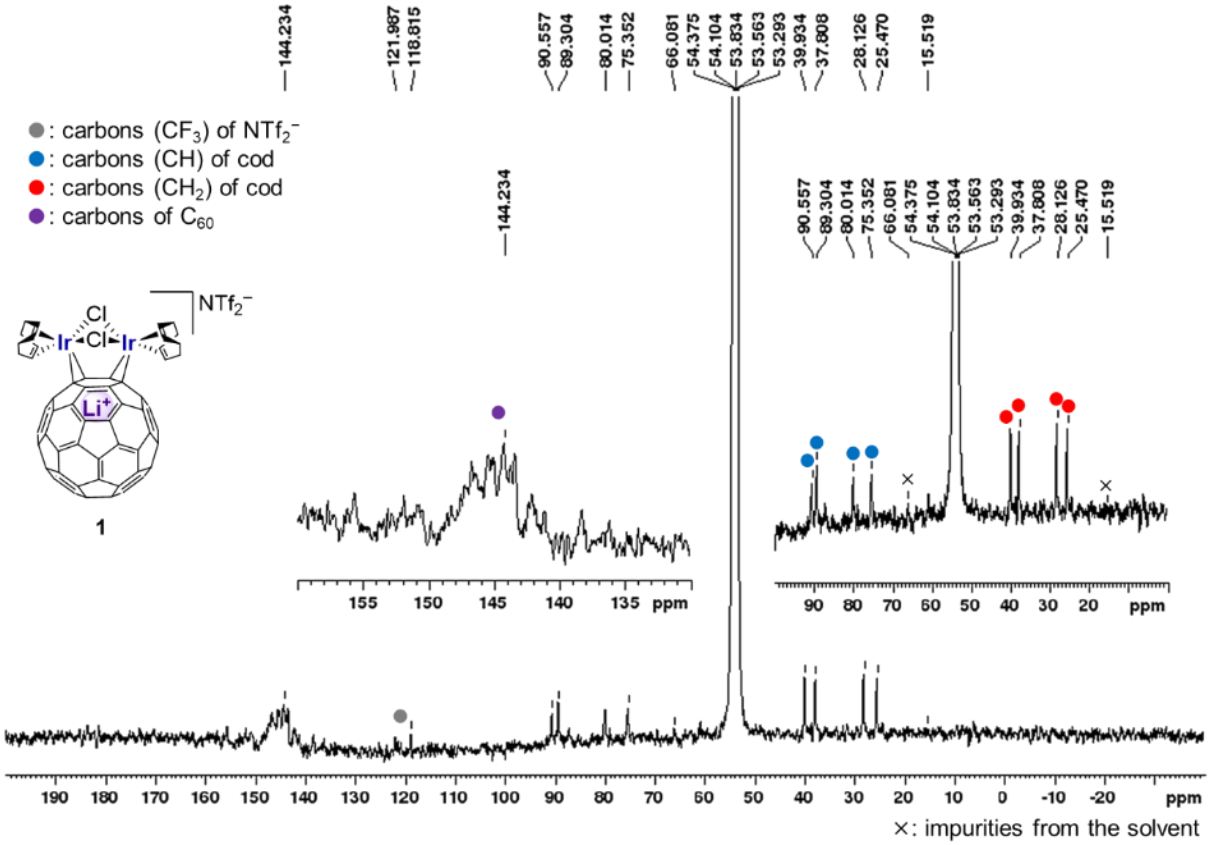

Fig. S8 $^{13}C\{^1H\}$ NMR spectrum of **1** (CD_2Cl_2, 101 MHz, 300 K).

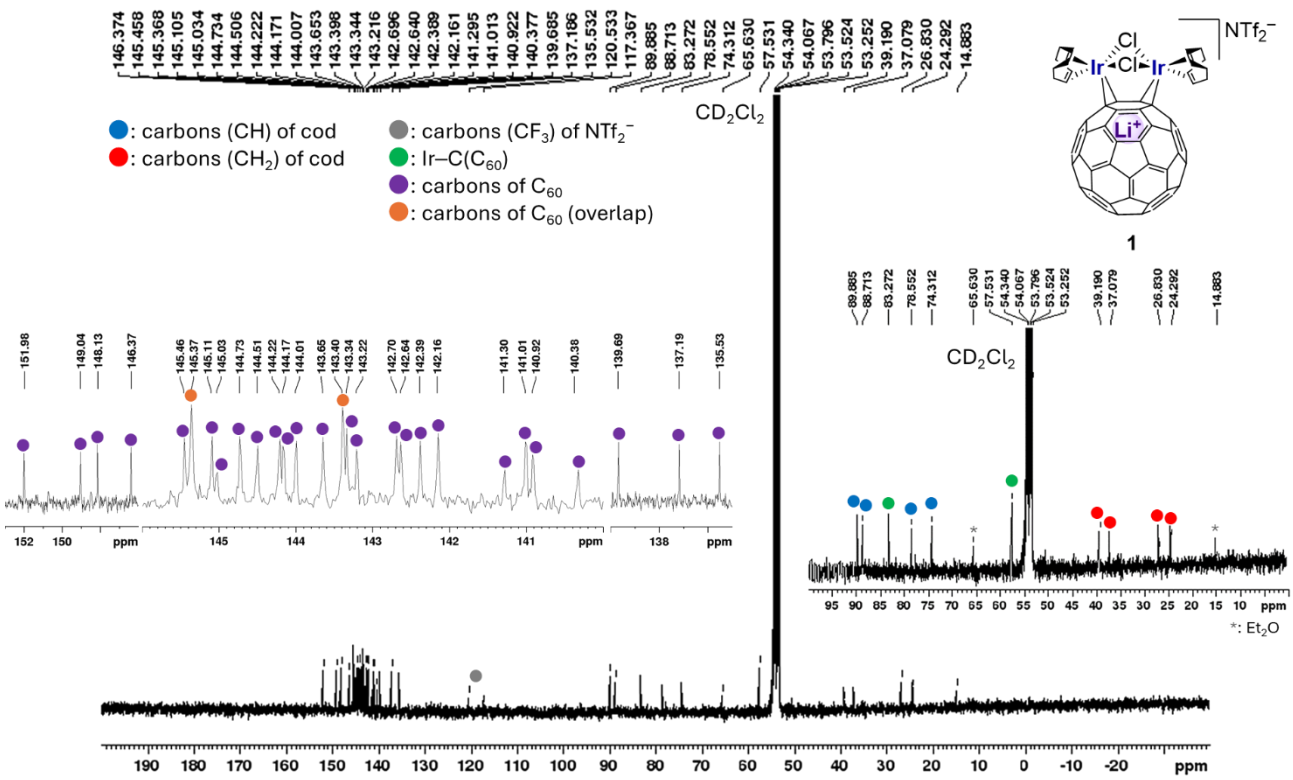

Fig. S9 $^{13}C\{^1H\}$ NMR spectrum of **1** (CD_2Cl_2, 101 MHz, 200 K).

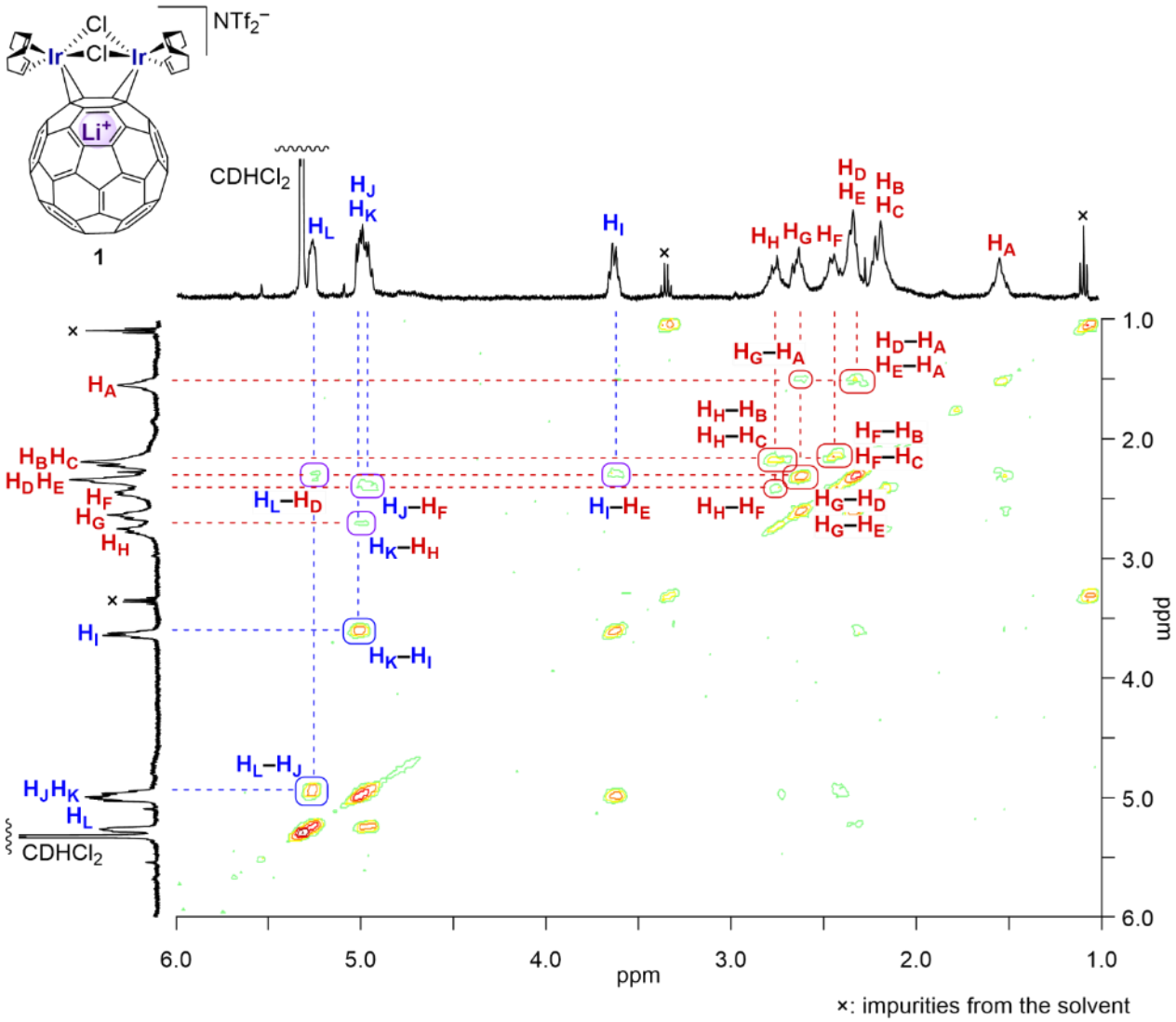

Fig. S10 ^{1}H–^{1}H COSY spectrum of **1** in CD_2Cl_2 (200 K).

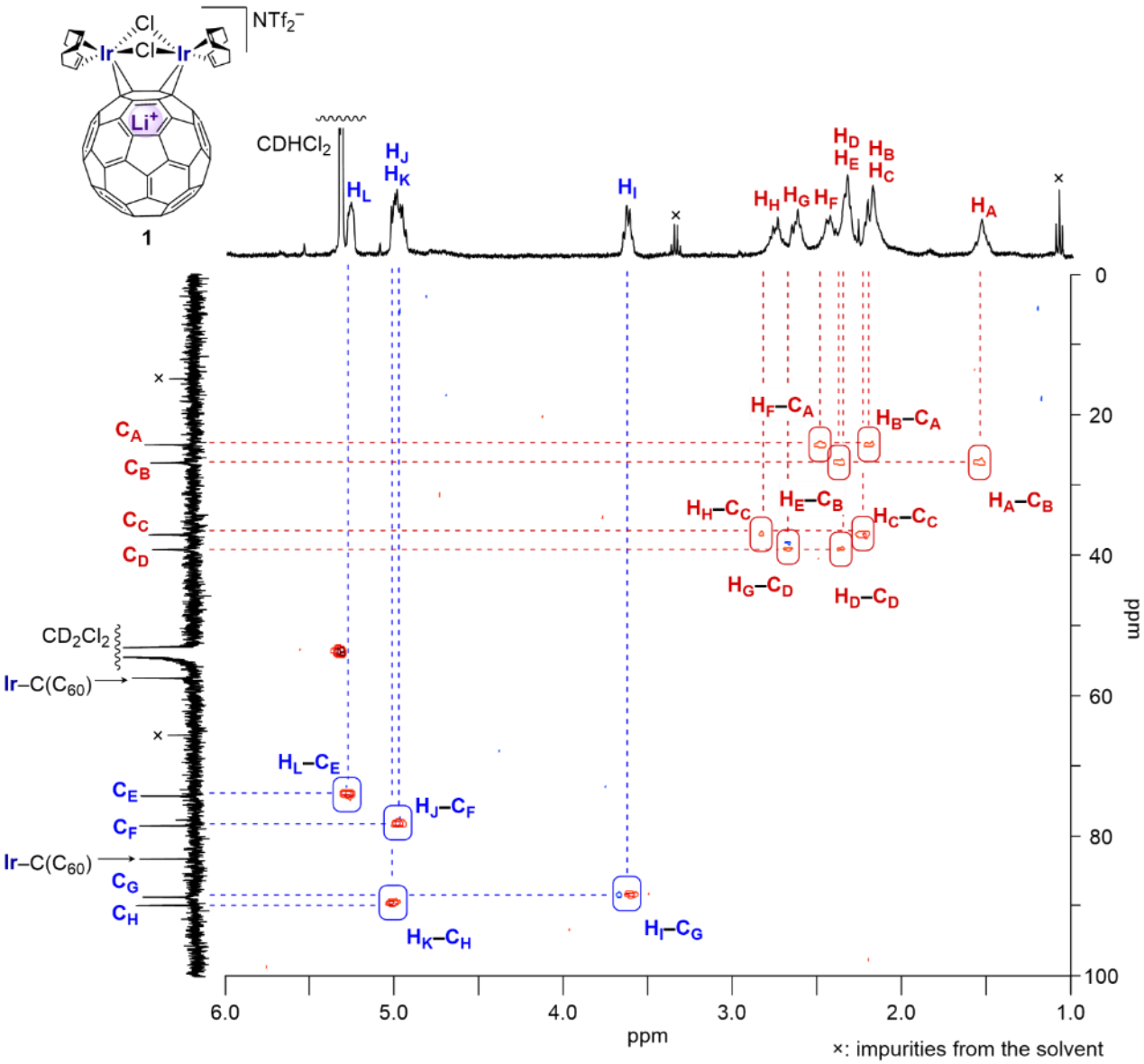

Fig. S11 ^{1}H–^{13}C HSQC spectrum of **1** in CD_2Cl_2 (200 K).

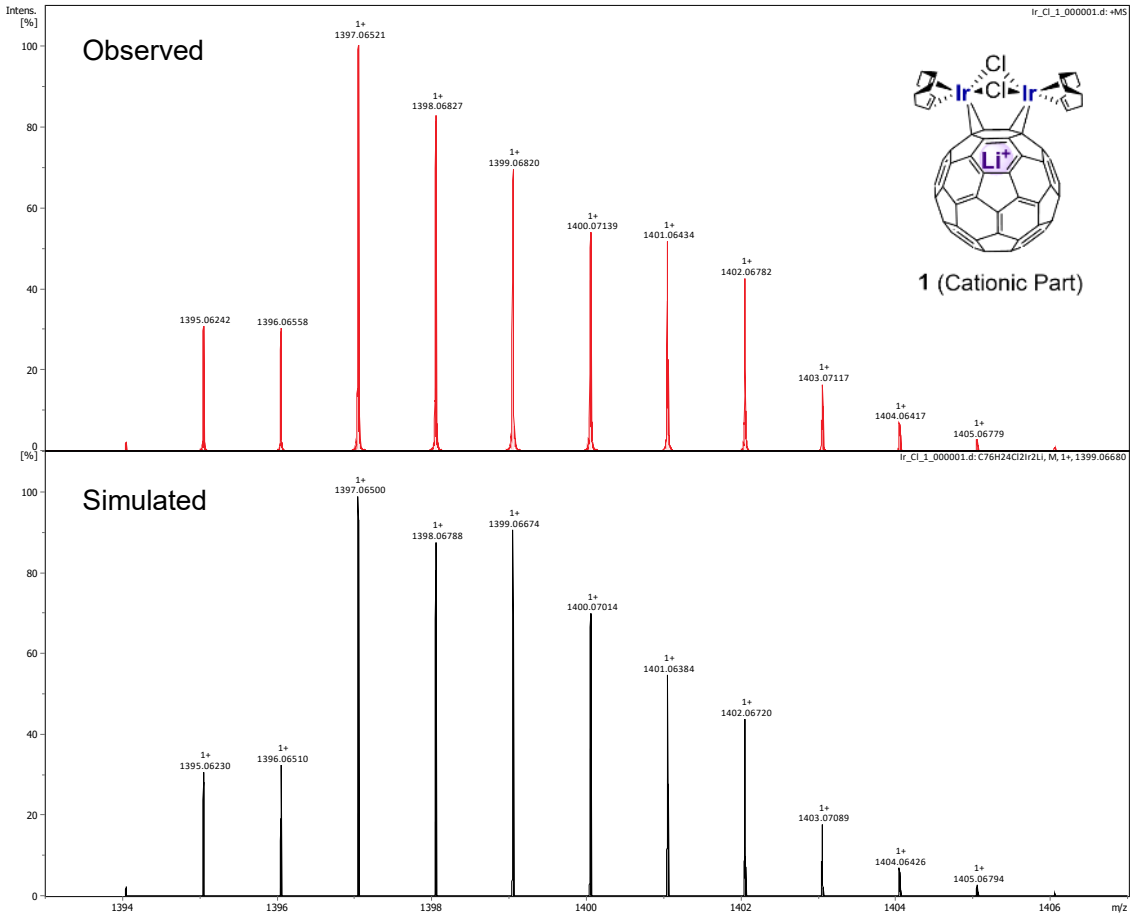

Fig. S12 HRMS (ESI) spectrum of **1** (upper) and the calculated distribution pattern of the cationic part $[C_{76}H_{24}LiCl_2Ir_2]^+$ (lower).

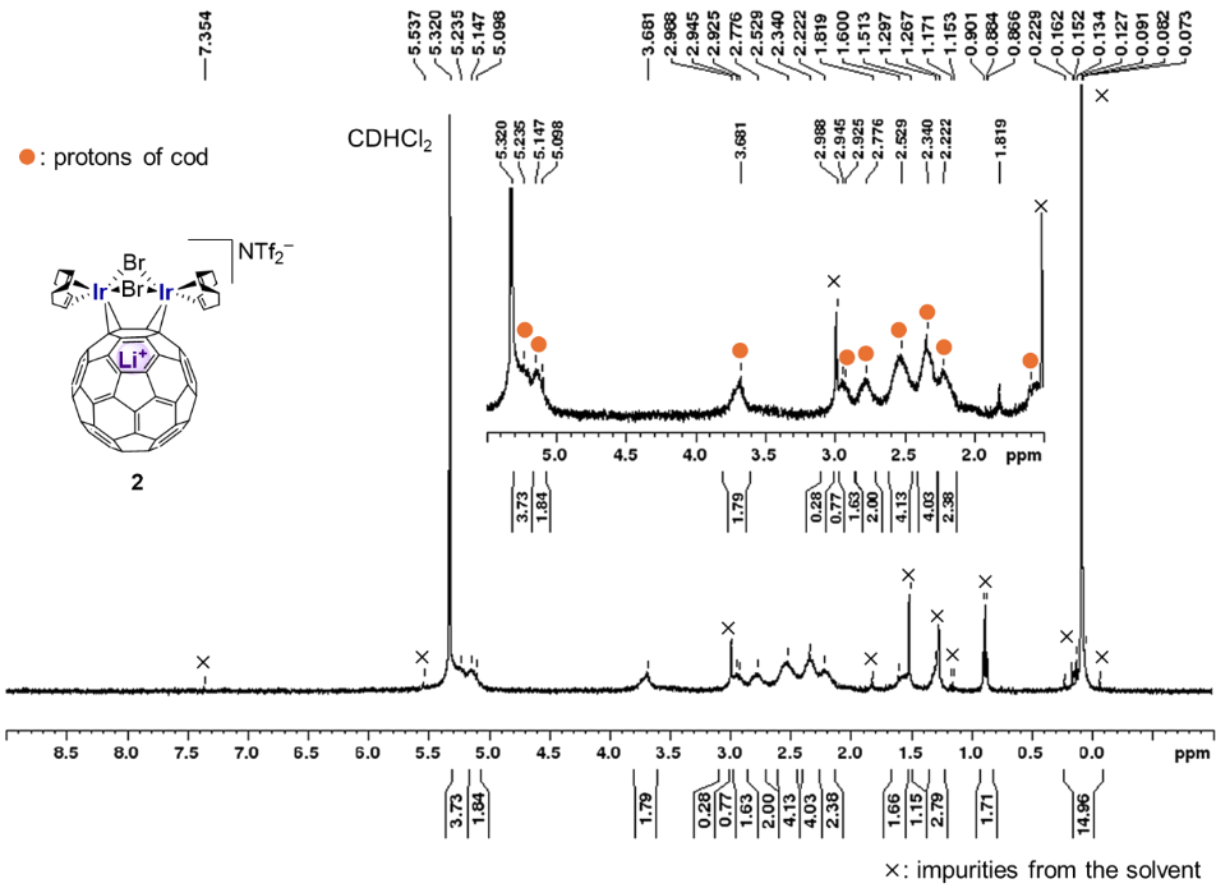

Fig. S13 ^{1}H NMR spectrum of [{μ-η^2:η^2-(Li$^+$@C$_{60}$)}{Ir$_2$Br$_2$(cod)$_2$}] (**2**) (CD$_2$Cl$_2$, 400 MHz, r.t.).

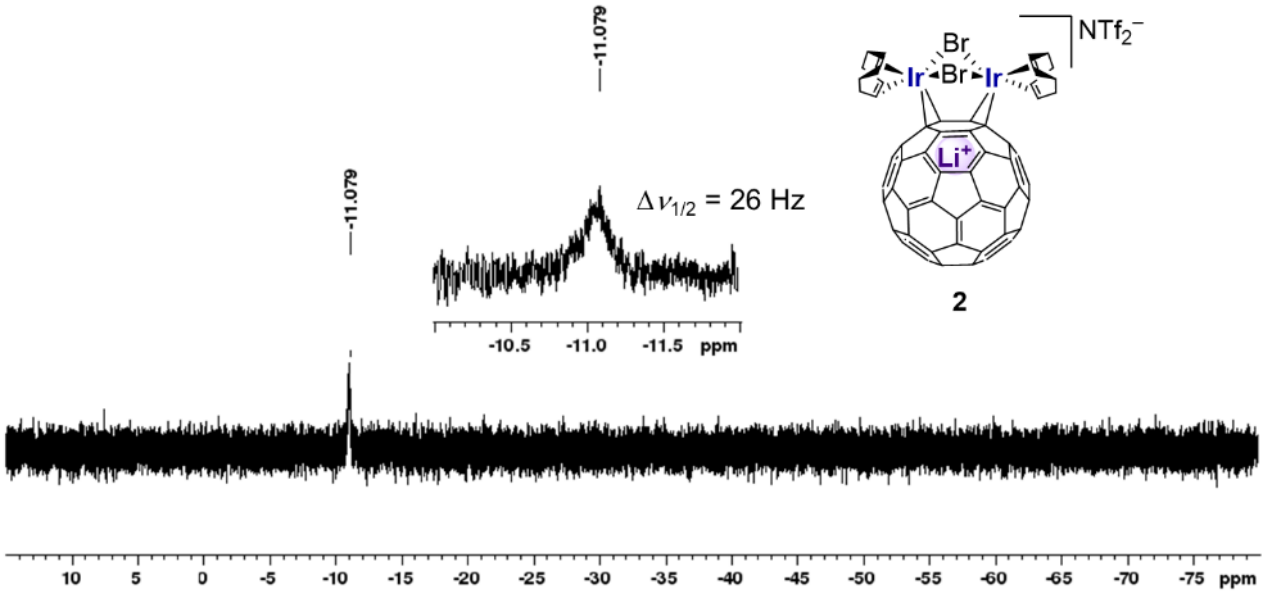

Fig. S14 ^{7}Li NMR spectrum of **2** (CD$_2$Cl$_2$, 156 MHz, r.t.).

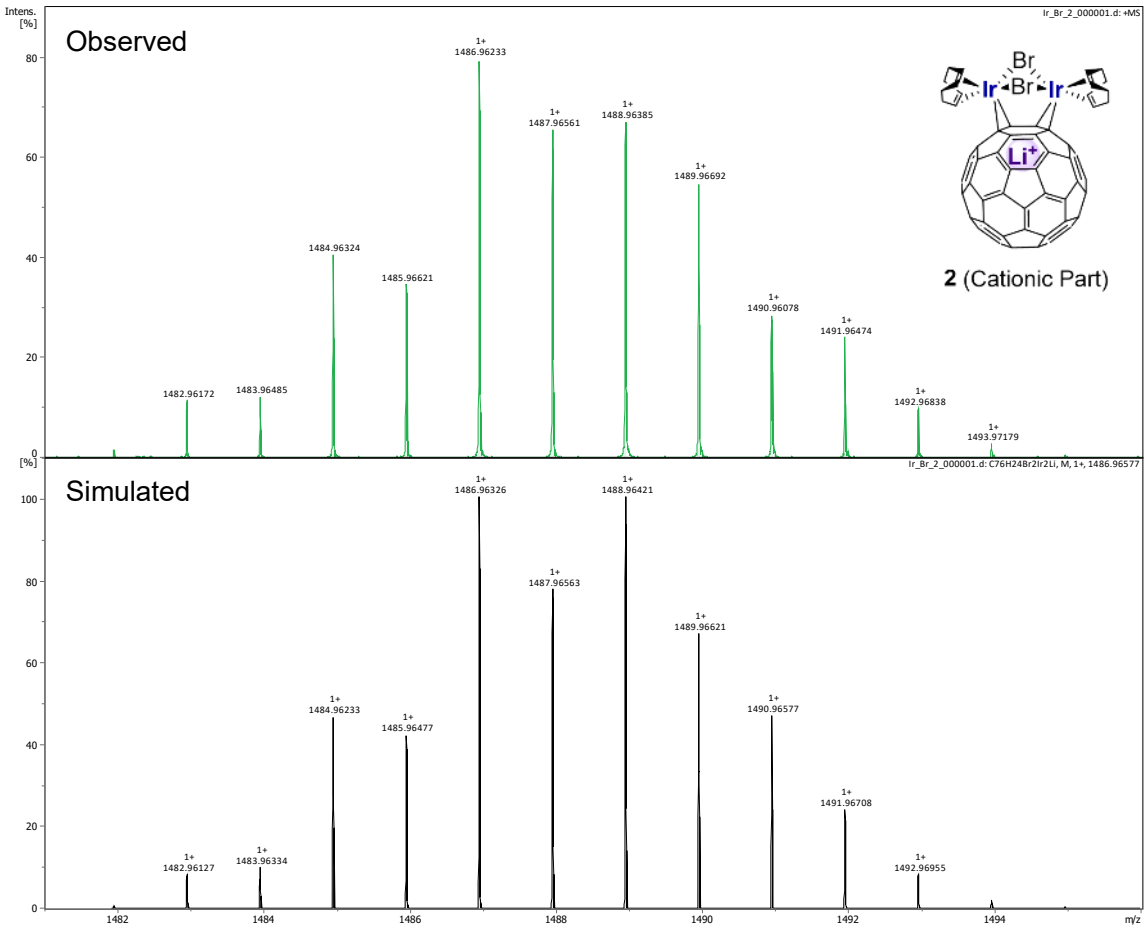

Fig. S15 HRMS (ESI) spectrum of **2** (upper) and the calculated distribution pattern of the cationic part $[C_{76}H_{24}LiBr_2Ir_2]^+$ (lower).

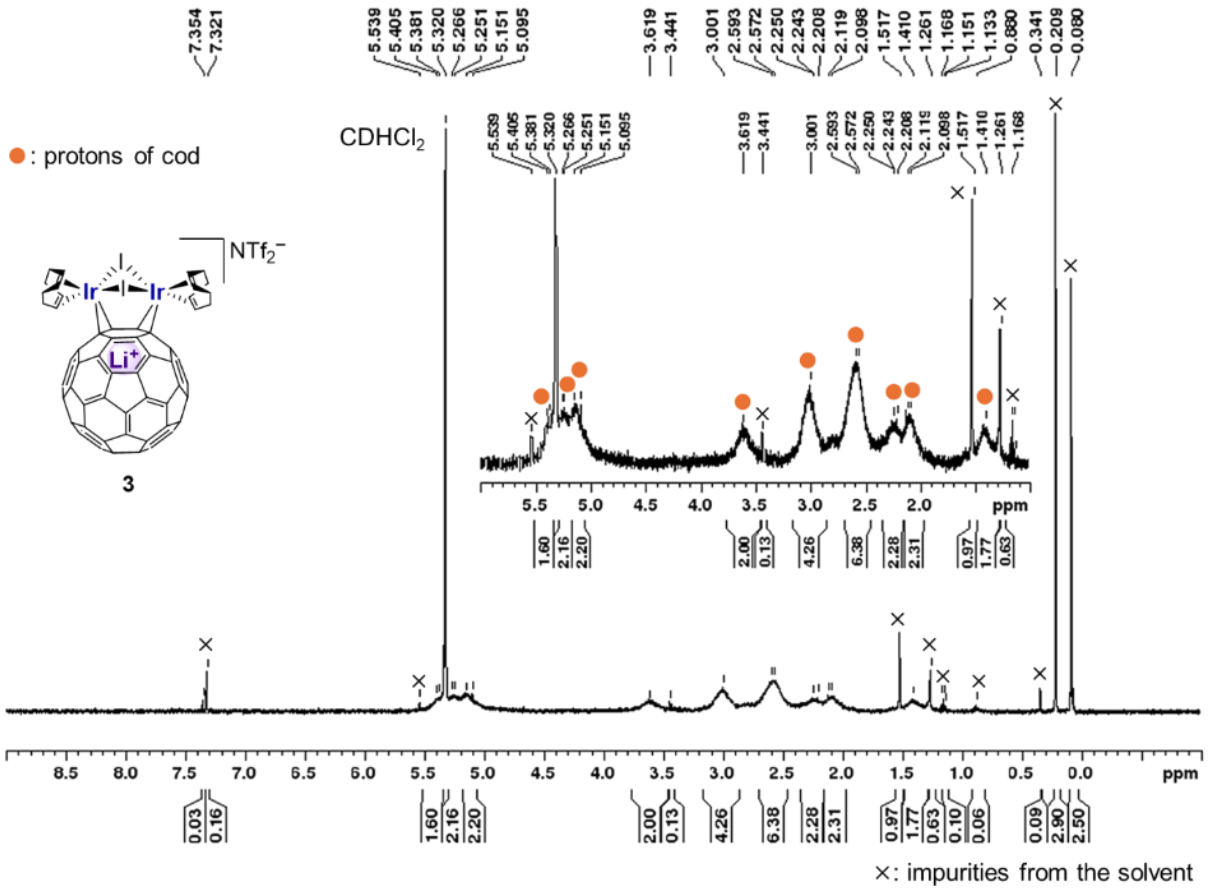

Fig. S16 ^{1}H NMR spectrum of [{μ-η^{2}:η^{2}-(Li^{+}@C_{60})}{$Ir_2I_2(cod)_2$}] (**3**) (CD_2Cl_2, 400 MHz, r.t.).

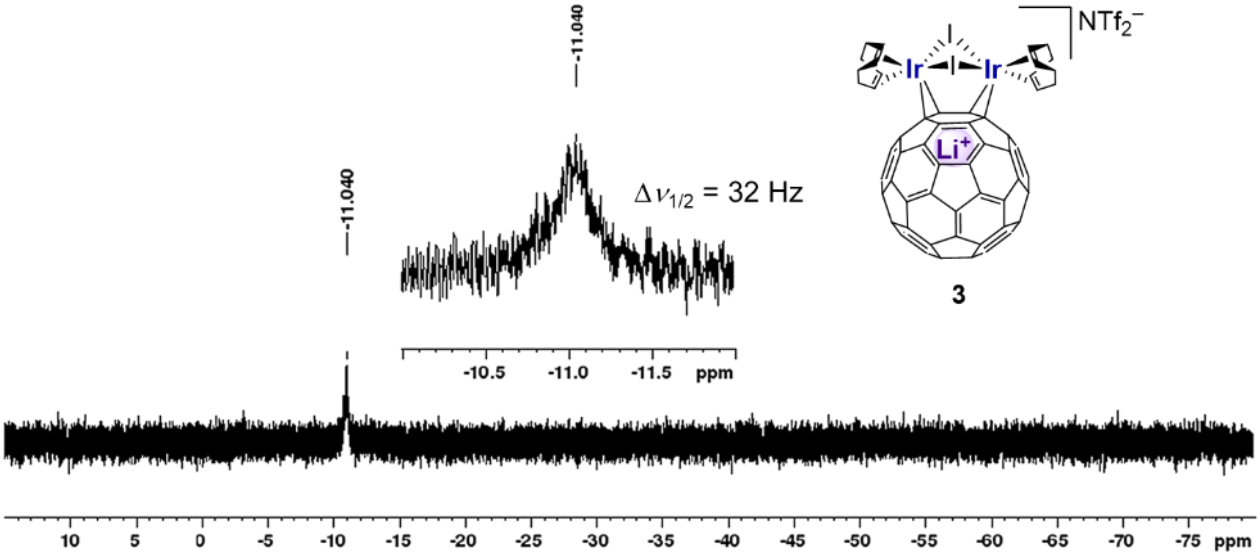

Fig. S17 ^{7}Li NMR spectrum of **3** (CD_2Cl_2, 156 MHz, r.t.).

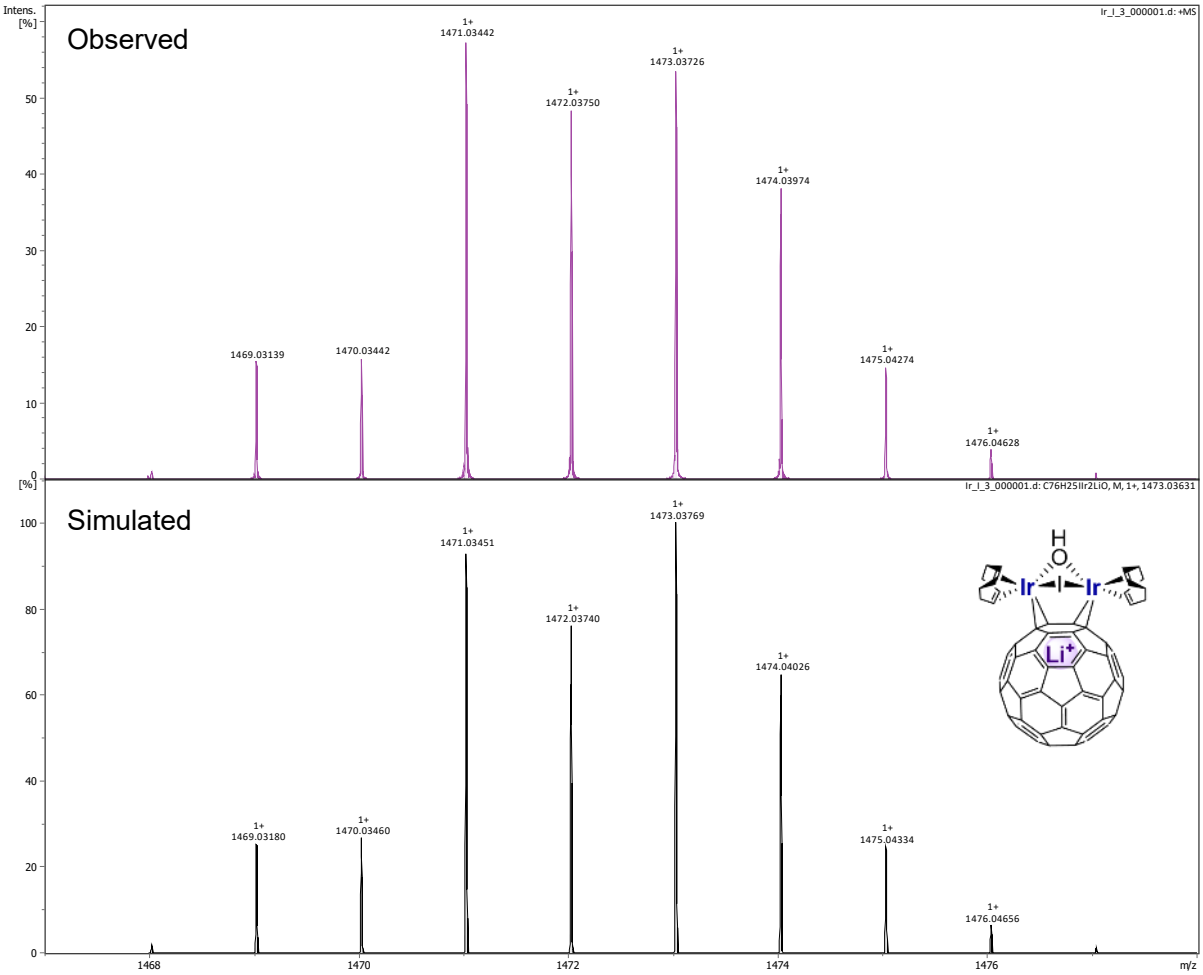

Fig. S18 HRMS (ESI) spectrum obtained from a solution of **3** (upper) and the calculated distribution pattern of the cation $[(Li^{+}@C_{60})\{Ir_2I(OH)(cod)_2\}]^{+}$ ($[C_{76}H_{25}LiIOIr_2]^{+}$) (lower).

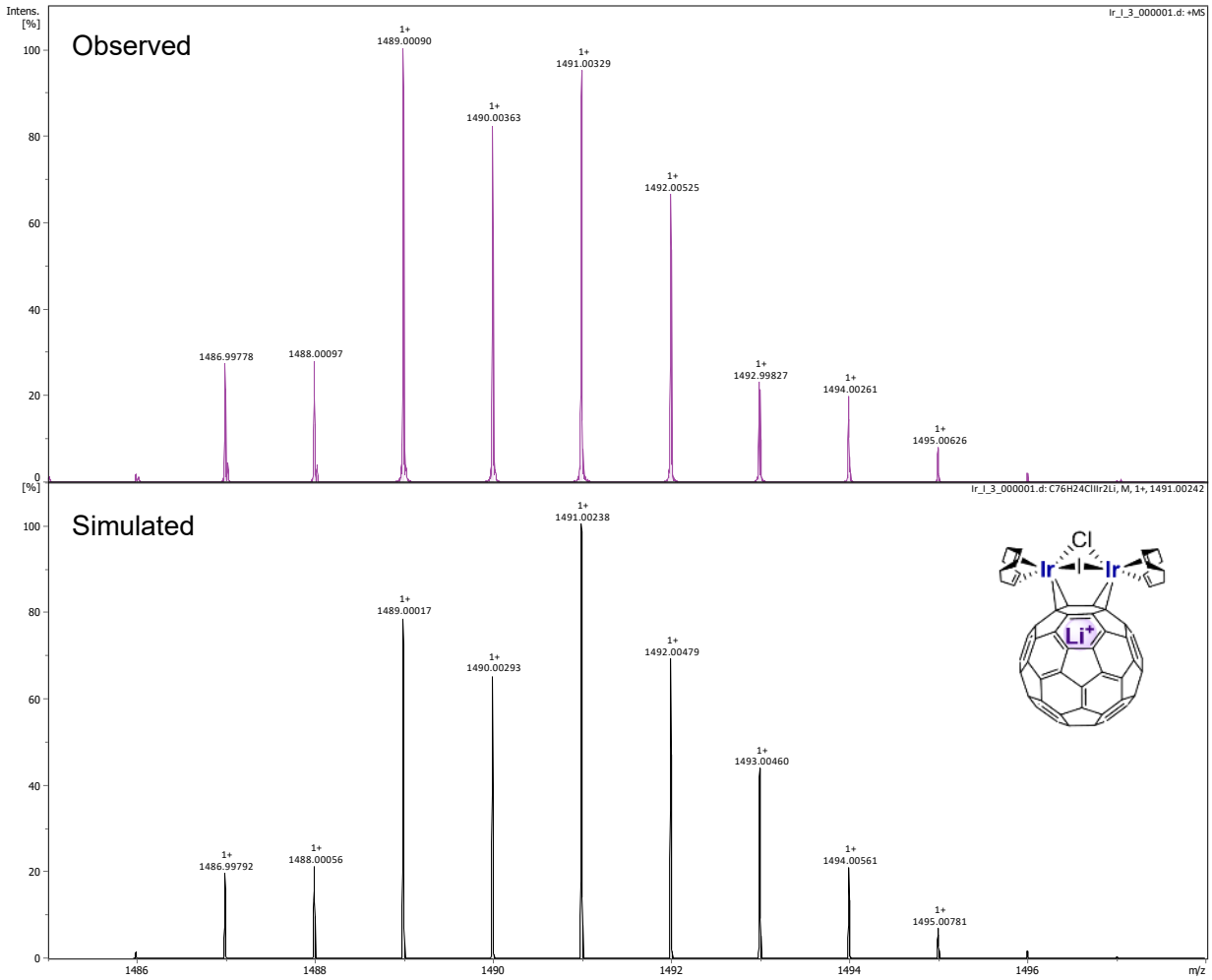

Fig. S19 HRMS (ESI) spectrum obtained from a solution of **3** (upper) and the calculated distribution pattern of the cation $[(Li^{+}@C_{60})\{Ir_2ICl(cod)_2\}]^{+}$ ($[C_{76}H_{24}LiIClIr_2]^{+}$) (lower).

4. UV/Vis spectra of complexes 1–3

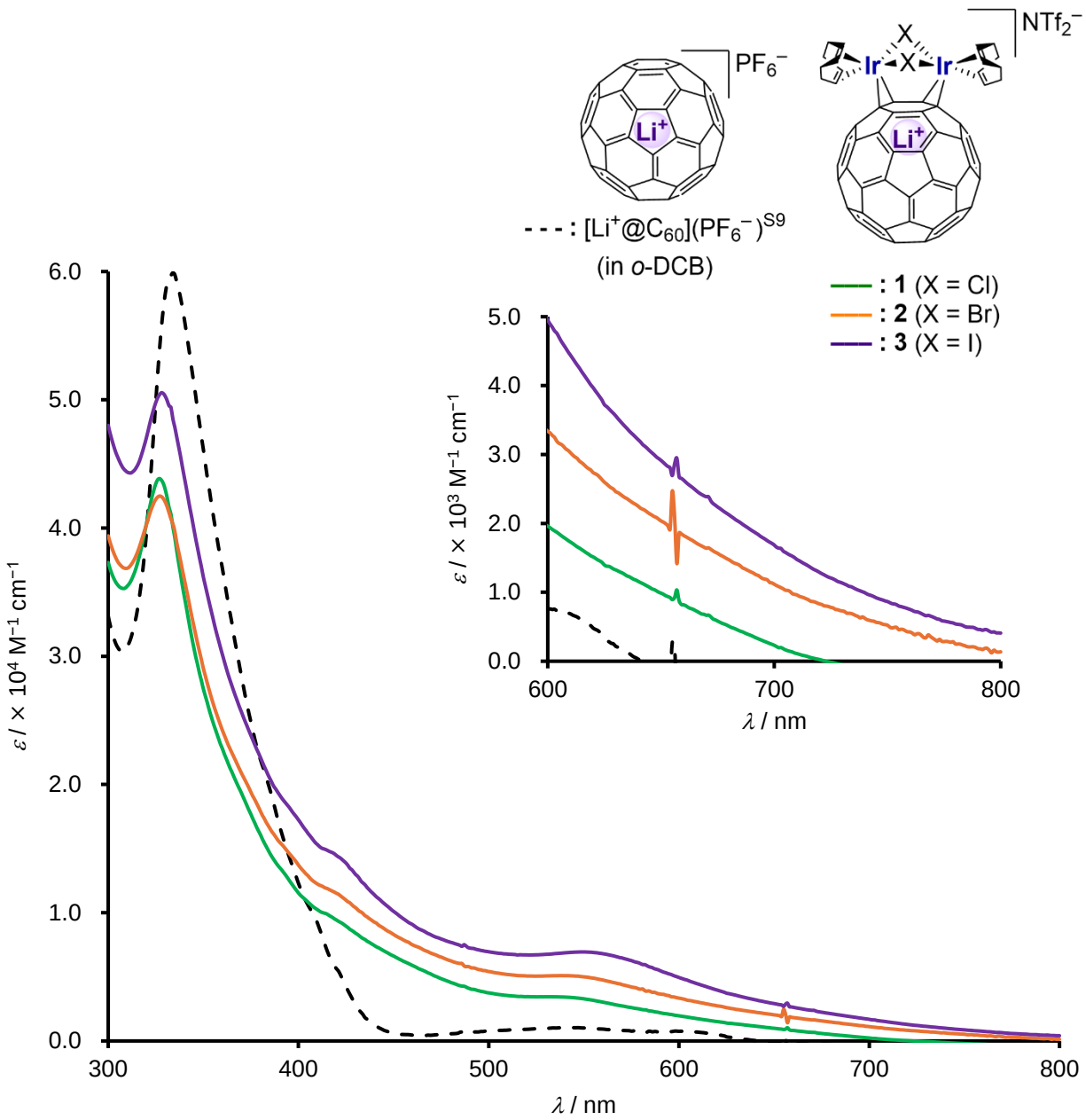

Fig. S20 UV/Vis absorption spectra of complexes **1**–**3** in CH_2Cl_2 at room temperature (1.0×10^{-4} M, 1 mm quartz cell). The corresponding spectrum of $[Li^+@C_{60}](PF_6^-)$[S9] in *o*-DCB is also shown as a reference.

5. Electrochemistry of complexes 1–3 and $Ir_2X_2(cod)_2$

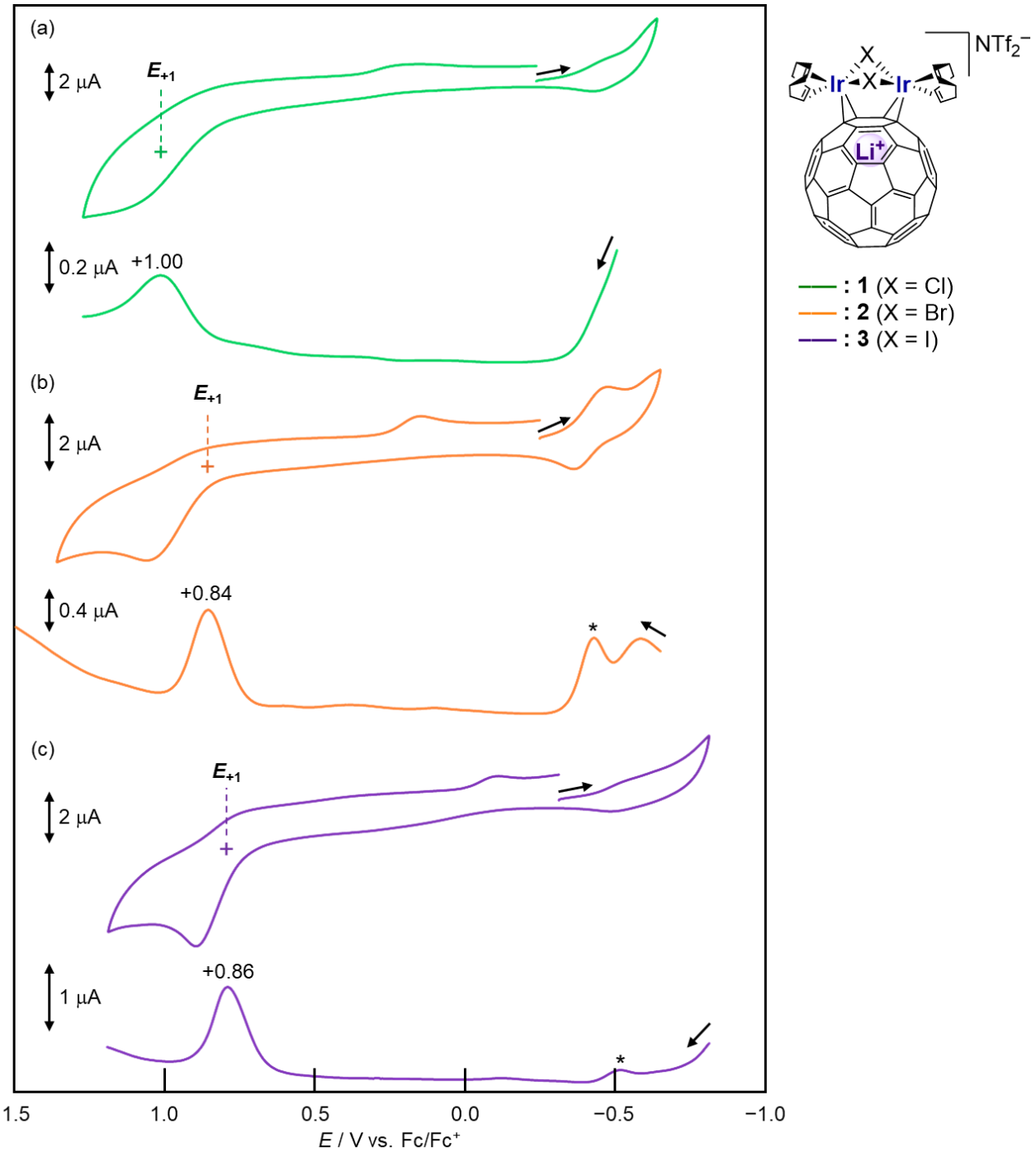

Fig. S21 Cyclic and differential pulse voltammograms (CV and DPV) of complexes (a) **1**, (b) **2** and (c) **3** in *o*-DCB with 200 mM (for **1**) or 100 mM (for **2** and **3**) $[^nBu_4N^+](NTf_2^-)$ as the electrolyte at the scan rate of 50 mV·s^{-1} (oxidation side, *: waves of free $Li^+@C_{60}$ formed from **1**–**3** in the measurements). Plus signs (+) indicate half-wave potentials. All potentials are referenced against the ferrocene/ferrocenium (Fc/Fc^+) couple.

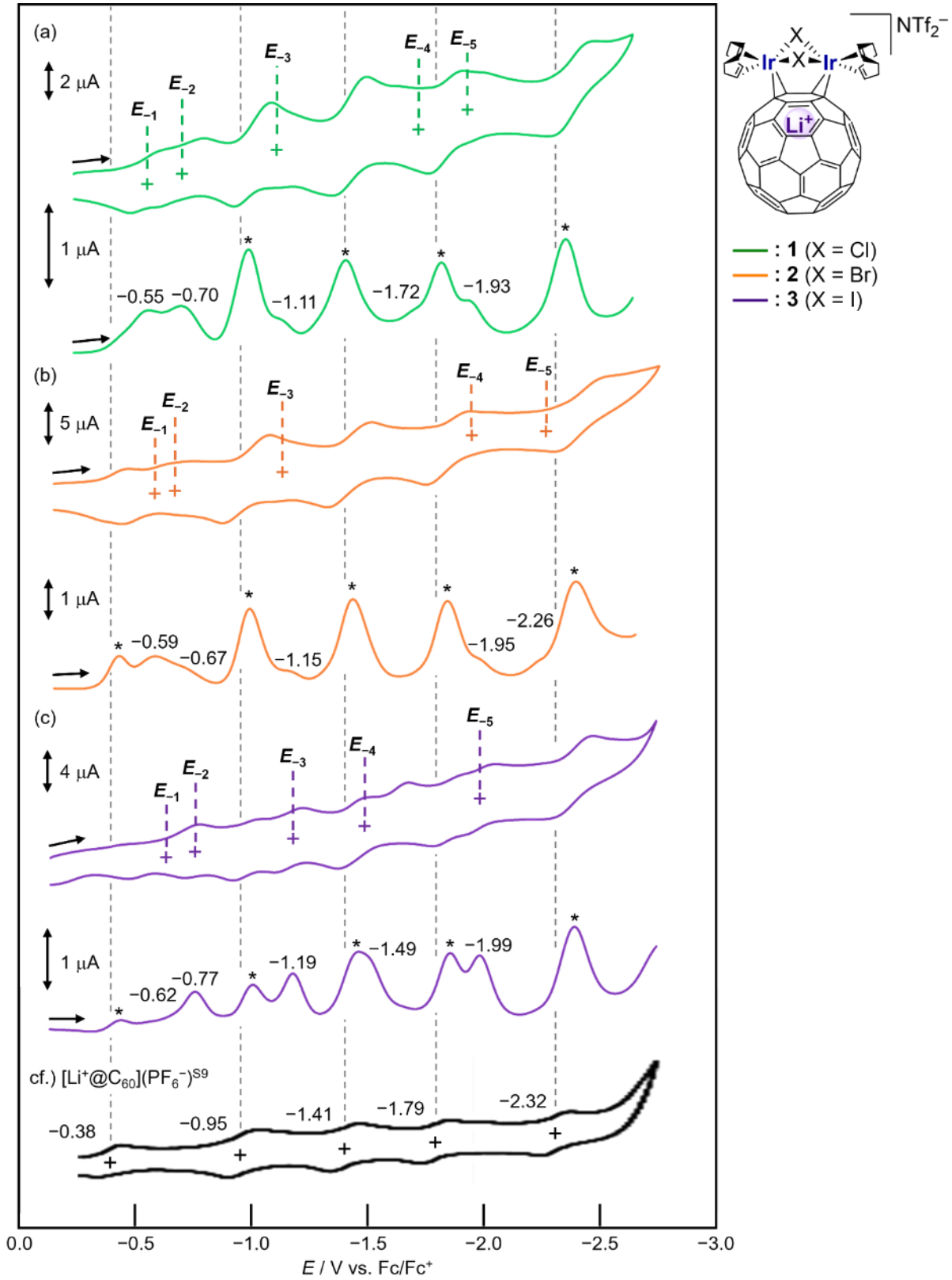

Fig. S22 CV and DPV of complexes (a) **1**, (b) **2** and (c) **3** in *o*-DCB with 200 mM (for **1**) or 100 mM (for **2** and **3**) [^{n}Bu$_4$N$^+$](NTf$_2^-$) as the electrolyte at the scan rate of 50 mV·s^{-1} (reduction side, *: waves of free Li$^+$@C$_{60}$ formed from **1**–**3** in the measurements). Plus signs (+) indicate half-wave potentials. All potentials are referenced against the ferrocene/ferrocenium (Fc/Fc$^+$) couple. CV of [Li$^+$@C$_{60}$](PF$_6^-$)^{S9} is shown at the bottom for a reference.

Table S3 The oxidation and reduction potentials of complexes **1**–**3**, $[Li^{+}@C_{60}](PF_6^{-})$[S9] and $Ir_2X_2(cod)_2$ (X = Cl, Br and I). All potentials were determined by the measurement of DPV (*: observed as shoulder peaks).

	E_{-5}	E_{-4}	E_{-3}	E_{-2}	E_{-1}	E_{+1}	E_{+2}	E_{+3}
1	−1.93*	−1.72*	−1.11*	−0.70	−0.55	+1.00	–	–
2	−2.26*	−1.95*	−1.15*	−0.67*	−0.59	+0.84	–	–
3	−1.99	−1.49*	−1.19	−0.77	−0.62*	+0.86	–	–
$Li^{+}@C_{60}$[S9]	−2.32	−1.79	−1.41	−0.95	−0.38	–	–	–
$Ir_2Cl_2(cod)_2$	–	–	−2.07	−1.60	−1.20	−0.02	+0.26	+0.70
$Ir_2Br_2(cod)_2$	–	−2.48	−2.36	−1.30	−1.08	+0.03	+0.28	+0.74
$Ir_2I_2(cod)_2$	–	−2.28	−1.65	−1.36	−0.93	+0.10	+0.45	+0.64

6. DFT calculations

Theoretical calculations were carried out for the cationic parts of **1**–**3** using the Gaussian 16 rev C.02 program package.[S10] All geometries were optimised by the DFT method at the B3PW91[S11–S13] level. Initial structures for optimisation were taken from the XRD structures. The 6-31G(d)[S14–S16] basis set was employed for H, Li, C, Cl and Br atoms, and Lanl2DZ[S17] basis set for Ir and I atoms. Natural bond orbital (NBO) population analysis was carried out to calculate Wiberg bond indices[S18] (WBI) and Natural population analysis (NPA) charges[S19] using the NBO 7.0 program[S20] at the B3PW91 level: The 6-311+G(d,p)[S14–S16,S21] basis set was used for H, Li, C, Cl and Br atoms, and the SDD[S21] basis set for Ir and I atoms using Grimme's D3 dispersion force model[S23] for empirical dispersion force correction in the gas phase. For the calculations of single-point energy and NMR spectra and chemical shift values using the GIAO method,[S24] the same functional and basis set for the NBO analysis were used. The ^{1}H and ^{13}C chemical shifts are referenced to $SiMe_4$, where shielding tensors were calculated at the B3PW91-D3/6-311+G(d,p) level of theory. TD-DFT calculations were performed at the B3PW91 level: The 6-31+G(d,p) basis set was used for H, Li, C, Cl and Br atoms, and the def2-TZVP[S25,S26] basis set for Ir and I atoms. For the NMR and TD-DFT calculations, the solvent effect of CH_2Cl_2 was considered using the SMD model.[S27] Optimised structures, **1-opt**, **2-opt** and **3-opt** are illustrated in Figs. S23, S24 and S25, respectively.

6-1. Optimised structures of the cation parts of complexes 1–3: 1-opt, 2-opt and 3-opt

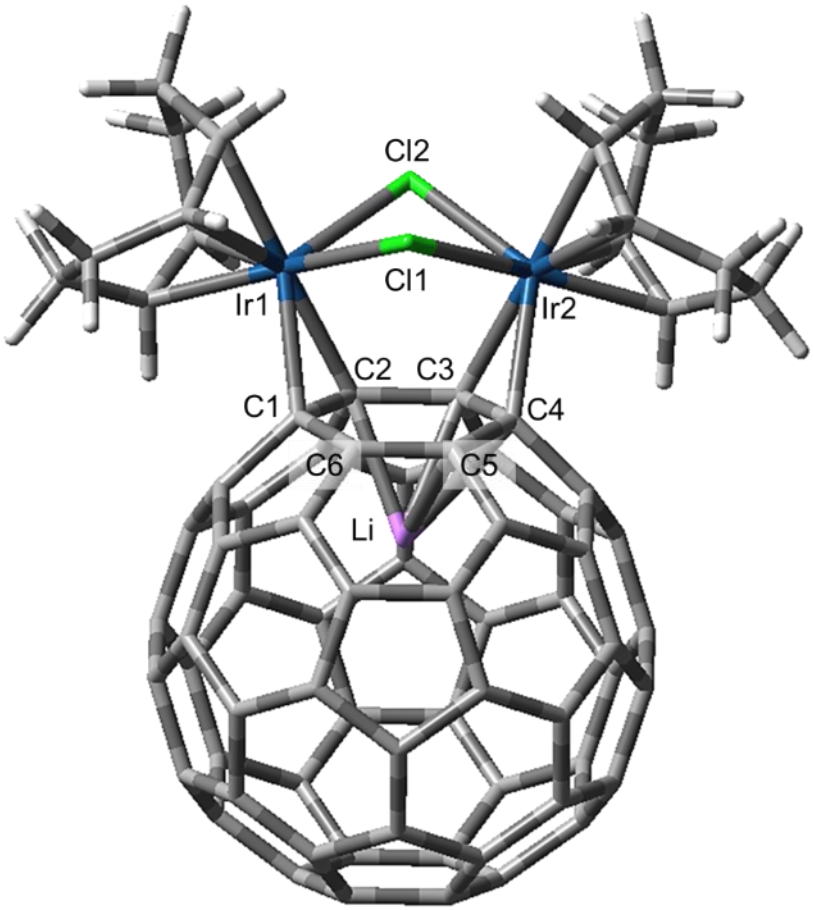

Fig. S23 Optimised structure of **1-opt**.

Table S4 Selected bond distances (Å) and angles (°) of **1-opt** and the crystal structure of **1**

	X-ray	Calcd.		X-ray	Calcd.
Ir1−Cl1	2.4025(9)	2.451	Li_A/Li_B−C1	2.69(7)/2.34(4)	2.398
Ir1−Cl2	2.5395(9)	2.592	Li_A/Li_B−C2	2.46(6)/2.22(4)	2.238
Ir2−Cl1	2.3955(9)	2.451	Li_A/Li_B−C3	2.22(3)/2.33(6)	2.238
Ir2−Cl2	2.5471(10)	2.592	Li_A/Li_B−C4	2.25(3)/2.56(7)	2.398
Ir1−C1	2.170(4)	2.191	Li_A/Li_B−C5	2.34(3)/2.50(5)	2.391
Ir1−C2	2.162(4)	2.176	Li_A/Li_B−C6	2.55(5)/2.40(4)	2.391
Ir2−C3	2.169(4)	2.176	Ir1−Cl1−Ir2	92.12(3)	91.91
Ir2−C4	2.170(4)	2.191	Ir1−Cl2−Ir2	85.56(3)	85.65
C1−C2	1.488(5)	1.499	Cl1−Ir1−Cl2	78.30(3)	78.37
C2−C3	1.531(5)	1.538	Cl1−Ir2−Cl2	78.27(3)	78.37
C3−C4	1.499(5)	1.499			
C4−C5	1.497(5)	1.502			
C5−C6	1.385(5)	1.391			
C6−C1	1.499(5)	1.502			

Table S5 Optimised atomic coordinates of **1-opt**

Symbol	*x*	*y*	*z*
Ir	0.0142761	−0.0376930	−0.0380126
Ir	0.0216277	−0.0349871	3.4854998
Li	−1.0578226	−3.7108068	1.7287602
Cl	1.7218629	−0.0364009	1.7201597
Cl	−1.0519003	1.5347145	1.7247590
C	0.0378220	−2.2141348	0.2096216
C	−1.1117638	−1.6105280	0.9584572
C	−1.1085637	−1.6093527	2.4961011
C	0.0441261	−2.2118201	3.2410653
C	1.0881589	−2.9126611	2.4191837
C	1.0852570	−2.9137289	1.0282375
C	1.6490905	0.3221707	−1.4128694
C	1.1201936	1.5695734	−0.9622585
C	0.2608515	2.4948355	−1.8147824
C	−1.2408806	2.2358681	−1.6086698
C	−1.5510106	0.7902391	−1.2940620
C	−0.9939272	−0.3156708	−1.9698289
C	−0.0725385	−0.2232628	−3.1768656
C	1.4061829	−0.2796232	−2.7766891
C	1.1314970	1.5736731	4.4026062
C	1.6623129	0.3269466	4.8528365
C	1.4251802	−0.2729577	6.2184928
C	−0.0517602	−0.2156887	6.6249827
C	−0.9783037	−0.3100013	5.4220586
C	−1.5382810	0.7948401	4.7469365
C	−1.2268375	2.2409619	5.0579705
C	0.2757571	2.5002778	5.2572957
C	−0.2593050	−3.1884889	−0.8715289
C	−1.5553270	−3.4642992	−1.2855325
C	−2.6866154	−2.9007422	−0.5507956
C	−2.4599712	−2.0910566	0.5614747
C	−3.2803352	−2.2871146	1.7323131
C	−2.4551032	−2.0892658	2.8994291
C	−2.6771230	−2.8972341	4.0138804
C	−1.5427839	−3.4596720	4.7447671
C	−0.2484976	−3.1845120	4.3249378
C	0.7144369	−4.2567935	4.3029154
C	1.5386006	−4.0901569	3.1260586
C	2.0070568	−5.2145950	2.4428933
C	2.0040530	−5.2156972	1.0042373
C	1.5327555	−4.0923079	0.3213064
C	0.7037137	−4.2607409	−0.8518631
C	0.3650427	−5.5421522	−1.2927473
C	−0.9795826	−5.8121850	−1.7433898
C	−1.9256751	−4.7862022	−1.7311370
C	−3.2765499	−5.0494457	−1.2813751
C	−3.7429260	−3.8861910	−0.5522438
C	−4.5578825	−4.0459834	0.5675879
C	−4.3187130	−3.2327450	1.7351936
C	−4.5530093	−4.0441946	2.9050256
C	−3.7333953	−3.8826908	4.0212036
C	−3.2639968	−5.0448251	4.7501765
C	−1.9112697	−4.7808991	5.1939205
C	−0.9651357	−5.8068680	5.2037904
C	0.3776023	−5.5375277	4.7471539
C	0.8513294	−6.7032120	4.0255143
C	1.6526681	−6.5446585	2.8974329
C	1.4276703	−7.3684043	1.7264112
C	1.6477771	−6.5464463	0.5532098
C	0.8417710	−6.7067309	−0.5712977
C	−0.2171699	−7.6938025	−0.5717803
C	−1.3456651	−7.1386916	−1.2958226
C	−2.6450884	−7.3908210	−0.8583601
C	−3.6301947	−6.3266772	−0.8540160
C	−4.4690067	−6.4931286	0.3182602
C	−4.9263316	−5.3743776	1.0132452
C	−4.9233038	−5.3732645	2.4629389
C	−4.4630942	−6.4909475	3.1577268
C	−3.6194219	−6.3227102	4.3262569
C	−2.6343056	−7.3868515	4.3281271
C	−1.3330736	−7.1340545	4.7597837
C	−0.2075971	−7.6902749	4.0319075
C	−0.4297293	−8.4777364	2.9035965
C	0.4040435	−8.3149674	1.7292627
C	−0.4346071	−8.4795240	0.5586568
C	−1.7863613	−8.7430917	1.0096701
C	−2.8698646	−8.2091664	0.3146093
C	−3.9961918	−7.6540158	1.0407332
C	−3.9932851	−7.6529405	2.4350753
C	−2.8639542	−8.2069952	3.1573629
C	−1.7833493	−8.7419906	2.4586163
H	2.5728980	−0.0087184	−0.9370655
H	1.6833343	2.0633448	−0.1717560
H	0.4839579	3.5309940	−1.5426402
H	0.5389290	2.3979650	−2.8695234
H	−1.6046218	2.8454444	−0.7759306
H	−1.8253149	2.5392065	−2.4906892
H	−2.4969627	0.6233216	−0.7788542
H	−1.5797948	−1.2250675	−1.9184969
H	−0.3026581	−1.0522301	−3.8542549
H	−0.2974394	0.6915360	−3.7339784
H	2.0396590	0.2174828	−3.5261802
H	1.7335599	−1.3246216	−2.7451869
H	1.6912474	2.0661971	3.6089251
H	2.5840677	−0.0046634	4.3735638
H	1.7520779	−1.3180992	6.1868647
H	2.0620542	0.2249137	6.9645871
H	−0.2741183	0.7000765	7.1815226
H	−0.2790701	−1.0434895	7.3047443
H	−1.5643302	−1.2195068	5.3746249
H	−2.4864380	0.6271143	4.2360653
H	−1.5941267	2.8492286	4.2258292
H	−1.8075226	2.5456771	5.9419887
H	0.4976828	3.5360005	4.9825421
H	0.5583178	2.4051080	6.3109999

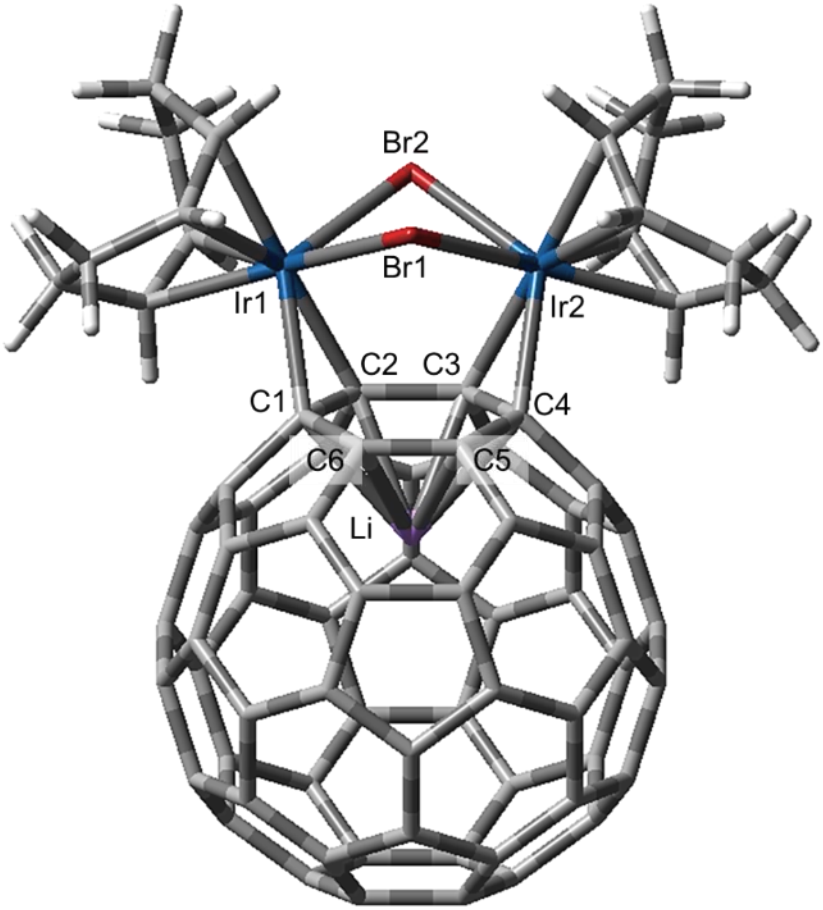

Fig. S24 Optimised structure of **2-opt**.

Table S6 Selected bond distances (Å) and angles (°) of **2-opt** and the crystal structure of **2**

	X-ray	Calcd.		X-ray	Calcd.
Ir1−Br1	2.5269(5)	2.545	Li_A/Li_B−C1	2.38(4)/2.81(9)	2.395
Ir1−Br2	2.6428(5)	2.674	Li_A/Li_B−C2	2.26(3)/2.52(8)	2.244
Ir2−Br1	2.5255(5)	2.545	Li_A/Li_B−C3	2.32(4)/2.23(5)	2.244
Ir2−Br2	2.6489(5)	2.674	Li_A/Li_B−C4	2.51(5)/2.28(5)	2.395
Ir1−C1	2.177(4)	2.200	Li_A/Li_B−C5	2.45(4)/2.45(5)	2.387
Ir1−C2	2.164(4)	2.178	Li_A/Li_B−C6	2.40(3)/2.68(8)	2.388
Ir2−C3	2.166(4)	2.178	Ir1−Br1−Ir2	89.012(17)	89.89
Ir2−C4	2.169(4)	2.200	Ir1−Br2−Ir2	84.023(15)	84.49
C1−C2	1.494(6)	1.500	Br1−Ir1−Br2	79.330(16)	79.37
C2−C3	1.542(6)	1.543	Br1−Ir2−Br2	79.237(17)	79.37
C3−C4	1.489(6)	1.500			
C4−C5	1.510(6)	1.503			
C5−C6	1.372(7)	1.391			
C6−C1	1.502(7)	1.503			

Table S7 Optimised atomic coordinates of **2-opt**

Symbol	*x*	*y*	*z*
Ir	0.0001386	0.0002182	0.0000809
Ir	0.0000482	0.0001674	3.5955295
Li	3.8240755	−0.0000586	1.7980954
Br	−1.2542046	1.5315145	1.7977984
Br	−0.5270304	−1.7222817	1.7977685
C	2.0851506	−0.6414326	0.2813309
C	1.8141807	0.6321846	1.0262551
C	1.8141323	0.6321698	2.5694569
C	2.0850643	−0.6414732	3.3143673
C	2.4702662	−1.8395451	2.4932812
C	2.4703072	−1.8395230	1.1024038
C	0.5715929	0.8915885	−1.9374453
C	−0.3311203	1.7460587	−1.2731625
C	−1.8009428	1.8645525	−1.6052017
C	−2.4808811	0.5001142	−1.8080129
C	−1.8490133	−0.5889540	−0.9491938
C	−0.8058115	−1.4585868	−1.3915714
C	−0.1416451	−1.4000754	−2.7462244
C	0.2303132	0.0322486	−3.1449194
C	−0.3312908	1.7459693	4.8688090
C	0.5714056	0.8914948	5.5331076
C	0.2300842	0.0321152	6.7405411
C	−0.1418389	−1.4002026	6.3417893
C	−0.8059425	−1.4586852	4.9871043
C	−1.8491379	−0.5890548	4.5447058
C	−2.4810552	0.4999790	5.4035323
C	−1.8011293	1.8644332	5.2007870
C	3.1033176	−0.6269531	−0.7985473
C	3.7247280	0.5415638	−1.2169458
C	3.4953851	1.7848473	−0.4829001
C	2.6544217	1.7925683	0.6292237
C	3.0702612	2.5295753	1.7979079
C	2.6543570	1.7925455	2.9665573
C	3.4952711	1.7847947	4.0787204
C	3.7245793	0.5414915	4.8127460
C	3.1031872	−0.6270173	4.3942915
C	3.8676304	−1.8485193	4.3743139
C	3.4774154	−2.5972048	3.1997924
C	4.4289899	−3.3586745	2.5169219
C	4.4290256	−3.3586566	1.0788212
C	3.4774870	−2.5971683	0.3959224
C	3.8677577	−1.8484558	−0.7785628
C	5.1920034	−1.8770523	−1.2219577
C	5.8217347	−0.6599895	−1.6759514
C	5.0962098	0.5324769	−1.6645430
C	5.7220189	1.7592664	−1.2174624
C	4.7332980	2.5290883	−0.4880494
C	5.1125400	3.2709082	0.6296112
C	4.2660599	3.2669985	1.7979468
C	5.1124828	3.2708800	2.9663248
C	4.7331853	2.5290355	4.0839498
C	5.7218700	1.7591955	4.8133932
C	5.0960391	0.5323946	5.2604126
C	5.8215628	−0.6600726	5.2718273
C	5.1918547	−1.8771250	4.8177735
C	6.1808355	−2.6553634	4.0963814
C	5.8058474	−3.3837172	2.9699778
C	6.6582806	−3.3964298	1.7979261
C	5.8059055	−3.3836898	0.6258325
C	6.1809482	−2.6553074	−0.5005341
C	7.4214968	−1.9092238	−0.5037993
C	7.1980348	−0.6726916	−1.2298838
C	7.7991966	0.5077751	−0.7953307
C	7.0478202	1.7480038	−0.7920923
C	7.4402624	2.5105607	0.3784735
C	6.4917675	3.2599565	1.0732407
C	6.4917322	3.2599393	2.5227629
C	7.4401925	2.5105268	3.2175595
C	7.0476920	1.7479420	4.3880873
C	7.7990680	0.5077128	4.3913329
C	7.1978858	−0.6727645	4.8258290
C	7.4213835	−1.9092795	4.0997261
C	8.2381031	−1.9145990	2.9703971
C	7.8502980	−2.6732889	1.7979647
C	8.2381611	−1.9145708	0.6255695
C	8.8645735	−0.6869576	1.0735611
C	8.6491002	0.5004773	0.3765956
C	8.4269700	1.7375981	1.1008051
C	8.4269364	1.7375818	2.4952586
C	8.6490308	0.5004435	3.2194494
C	8.8645376	−0.6869748	2.5224659
H	1.6107131	1.1894600	−1.8761634
H	0.1002043	2.6104576	−0.7684579
H	−1.9129572	2.5049508	−2.4932757
H	−2.2898333	2.3964397	−0.7830368
H	−2.4633707	0.2019806	−2.8616056
H	−3.5389150	0.5864163	−1.5419179
H	−2.4950831	−0.9909377	−0.1697951
H	−0.7703107	−2.4428733	−0.9231670
H	0.7670280	−2.0104704	−2.6997520
H	−0.7874664	−1.8691150	−3.5034489
H	1.0972039	0.0146748	−3.8137394
H	−0.5764419	0.5078741	−3.7114120
H	0.1000432	2.6103866	4.3641440
H	1.6105240	1.1893840	5.4718777
H	1.0969454	0.0145330	7.4093990
H	−0.5767023	0.5077147	7.3070113
H	0.7668430	−2.0105863	6.2953424
H	−0.7876901	−1.8692696	7.0989713
H	−0.7704068	−2.4429584	4.5186743
H	−2.4951706	−0.9910251	3.7652696
H	−2.4635795	0.2018148	6.4571172
H	−3.5390804	0.5862734	5.1373998
H	−1.9131908	2.5048049	6.0888742
H	−2.2899917	2.3963359	4.3786155

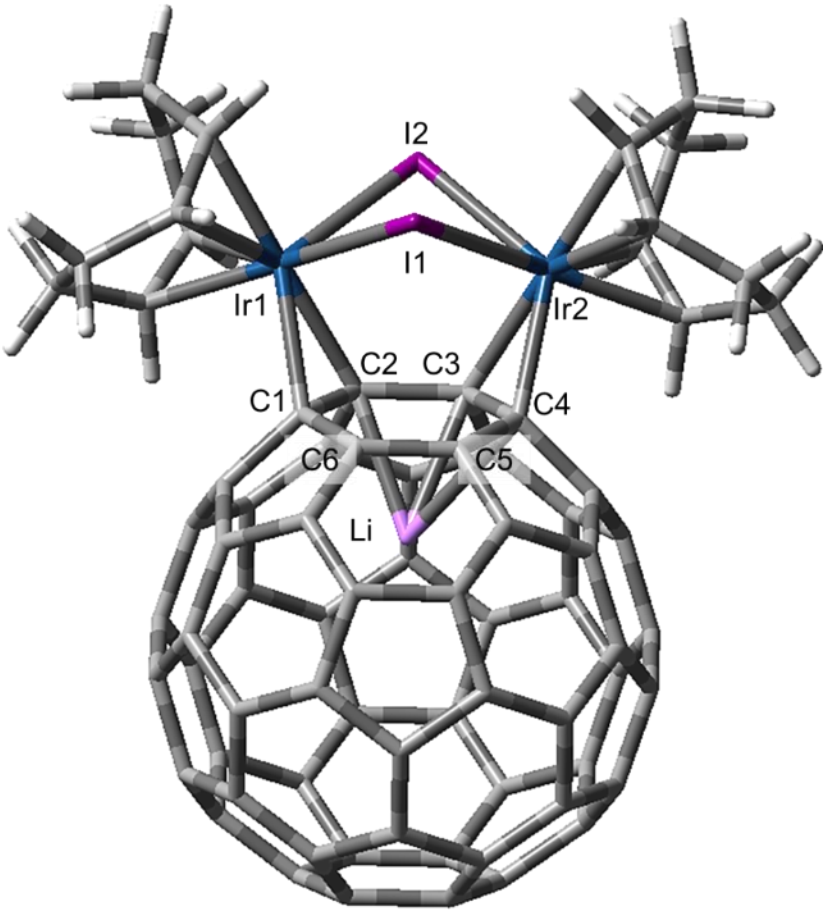

Fig. S25 Optimised structure of **3-opt**.

Table S8 Selected bond distances (Å) and angles (°) of **3-opt** and the crystal structure of **3**

	X-ray	Calcd.		X-ray	Calcd.
Ir1−I1	2.6877(8)	2.772	Li_A/Li_B−C1	2.38(5)/2.81(9)	2.397
Ir1−I2	2.7611(6)	2.878	Li_A/Li_B−C2	2.24(5)/2.57(8)	2.252
Ir2−I1	2.6747(7)	2.772	Li_A/Li_B−C3	2.29(5)/2.25(7)	2.252
Ir2−I2	2.7740(6)	2.878	Li_A/Li_B−C4	2.47(6)/2.20(7)	2.398
Ir1−C1	2.187(8)	2.209	Li_A/Li_B−C5	2.45(5)/2.32(8)	2.389
Ir1−C2	2.184(8)	2.198	Li_A/Li_B−C6	2.40(4)/2.60(9)	2.389
Ir2−C3	2.175(8)	2.198	Ir1−I1−Ir2	85.68(2)	85.56
Ir2−C4	2.185(8)	2.209	Ir1−I2−Ir2	82.402(17)	81.72
C1−C2	1.497(11)	1.500	I1−Ir1−I2	80.27(2)	79.70
C2−C3	1.535(11)	1.550	I1−Ir2−I2	80.26(2)	79.70
C3−C4	1.502(11)	1.500			
C4−C5	1.501(11)	1.503			
C5−C6	1.387(11)	1.391			
C6−C1	1.506(11)	1.503			

Table S9 Optimised atomic coordinates of **3-opt**

Symbol	*x*	*y*	*z*
Ir	−0.0086768	−0.0259692	−0.0695440
Ir	−0.0180502	−0.0245811	3.6964512
Li	3.8019774	−0.0215974	1.8223557
I	−1.4299642	1.6277113	1.8092708
I	−0.7368110	−1.9270302	1.8123726
C	2.0690744	−0.6761117	0.3012712
C	1.7821072	0.5963070	1.0427682
C	1.7782870	0.5969345	2.5924632
C	2.0615751	−0.6748374	3.3363792
C	2.4573472	−1.8706372	2.5155782
C	2.4607847	−1.8712333	1.1250399
C	0.6562941	0.9045208	−1.9644939
C	−0.2886183	1.7469240	−1.3470190
C	−1.7262457	1.8659002	−1.7945327
C	−2.3922051	0.5002007	−2.0280442
C	−1.8040902	−0.5947885	−1.1452276
C	−0.7355642	−1.4569557	−1.5387354
C	0.0067373	−1.3739177	−2.8500279
C	0.3921004	0.0656861	−3.2034153
C	−0.3044905	1.7493442	4.9711139
C	0.6375159	0.9075930	5.5938788
C	0.3674918	0.0696719	6.8321644
C	−0.0160282	−1.3702639	6.4780615
C	−0.7518538	−1.4544447	5.1631804
C	−1.8186007	−0.5927627	4.7638006
C	−2.4111505	0.5028435	5.6428750
C	−1.7443525	1.8684522	5.4113163
C	3.0962077	−0.6601271	−0.7713441
C	3.7180202	0.5076975	−1.1885805
C	3.4821411	1.7490088	−0.4545539
C	2.6320353	1.7559487	0.6515768
C	3.0450930	2.4940313	1.8199985
C	2.6262312	1.7568932	2.9869450
C	3.4708127	1.7508698	4.0973037
C	3.7030202	0.5101735	4.8335222
C	3.0833012	−0.6579885	4.4141287
C	3.8504276	−1.8774894	4.3986964
C	3.4657482	−2.6260083	3.2233600
C	4.4197989	−3.3880003	2.5445453
C	4.4233761	−3.3885916	1.1071093
C	3.4727102	−2.6271816	0.4229159
C	3.8632426	−1.8796243	−0.7511114
C	5.1885595	−1.9058537	−1.1922720
C	5.8171026	−0.6881004	−1.6458179
C	5.0887669	0.5025251	−1.6348044
C	5.7094528	1.7313128	−1.1871788
C	4.7166383	2.4976281	−0.4593893
C	5.0904592	3.2420091	0.6575865
C	4.2401220	3.2352568	1.8226711
C	5.0846511	3.2429548	2.9919597
C	4.7052693	2.4994959	4.1076746
C	5.6944431	1.7337854	4.8410341
C	5.0715283	0.5053678	5.2866005
C	5.7998002	−0.6852488	5.3021694
C	5.1735238	−1.9033648	4.8464841
C	6.1662513	−2.6798038	4.1283598
C	5.7956438	−3.4092989	3.0012637
C	6.6511156	−3.4203985	1.8313896
C	5.8014765	−3.4102595	0.6572619
C	6.1776997	−2.6816977	−0.4685760
C	7.4164752	−1.9324685	−0.4690906
C	7.1920366	−0.6968143	−1.1964518
C	7.7889175	0.4857537	−0.7608504
C	7.0343136	1.7241269	−0.7596698
C	7.4215177	2.4884659	0.4116094
C	6.4692247	3.2359282	1.1036778
C	6.4656142	3.2365132	2.5527334
C	7.4144453	2.4896327	3.2501526
C	7.0214125	1.7262499	4.4201172
C	7.7759849	0.4878776	4.4260548
C	7.1769554	−0.6943315	4.8596648
C	7.4050107	−1.9305788	4.1344376
C	8.2244284	−1.9340449	3.0070807
C	7.8413746	−2.6942065	1.8340574
C	8.2302668	−1.9350081	0.6623347
C	8.8521276	−0.7054093	1.1113077
C	8.6355244	0.4812322	0.4132677
C	8.4083455	1.7182745	1.1364324
C	8.4048777	1.7188509	2.5308868
C	8.6284507	0.4824012	3.2561900
C	8.8485257	−0.7048145	2.5602097
H	1.6853413	1.2118283	−1.8417092
H	0.1063604	2.6053586	−0.8048962
H	−1.7577287	2.4855291	−2.7039091
H	−2.2816261	2.4215874	−1.0327054
H	−2.3249674	0.2034284	−3.0802911
H	−3.4617943	0.5838045	−1.8123874
H	−2.5053787	−1.0143749	−0.4259705
H	−0.7338400	−2.4555078	−1.1011199
H	0.9147291	−1.9803916	−2.7613473
H	−0.5923315	−1.8340051	−3.6501767
H	1.2967902	0.0639860	−3.8203182
H	−0.3842095	0.5454175	−3.8080627
H	0.0930314	2.6073771	4.4302169
H	1.6670890	1.2150166	5.4758618
H	1.2692287	0.0685451	7.4533766
H	−0.4117304	0.5497902	7.4327481
H	0.8924318	−1.9767550	6.3943792
H	−0.6190128	−1.8297255	7.2756233
H	−0.7478415	−2.4533498	4.7263809
H	−2.5163285	−1.0130354	4.0414879
H	−2.3488681	0.2069988	6.6956856
H	−3.4797184	0.5860496	5.4220604
H	−1.7805679	2.4890478	6.3198559
H	−2.2960176	2.4231506	4.6460729

6-2. Frontier orbitals and energy levels of 1-opt, 2-opt and 3-opt

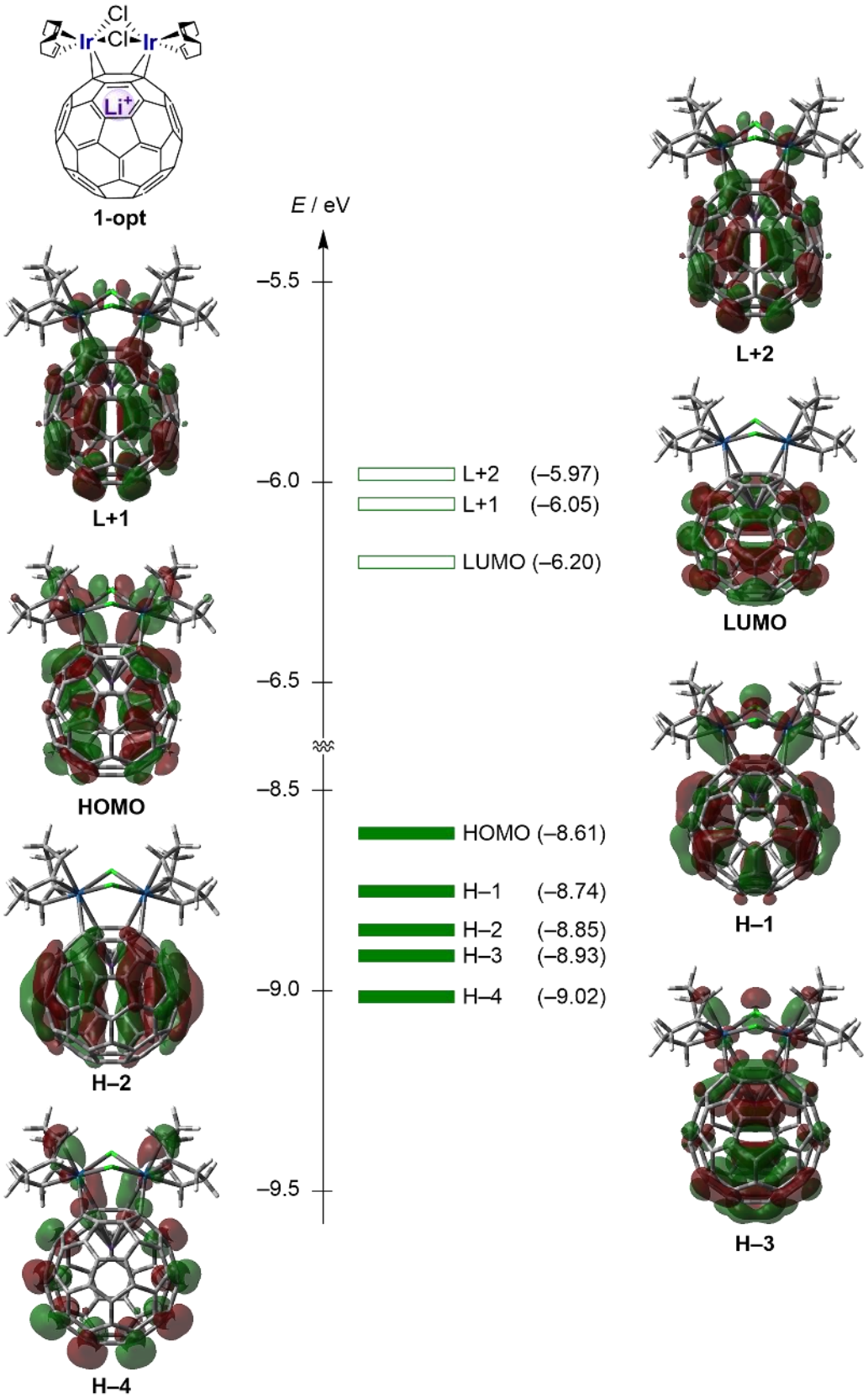

Fig. S26 Kohn-Sham orbitals and energy levels of **1-opt** (from LUMO+2 to HOMO−4, isovalue = 0.02).

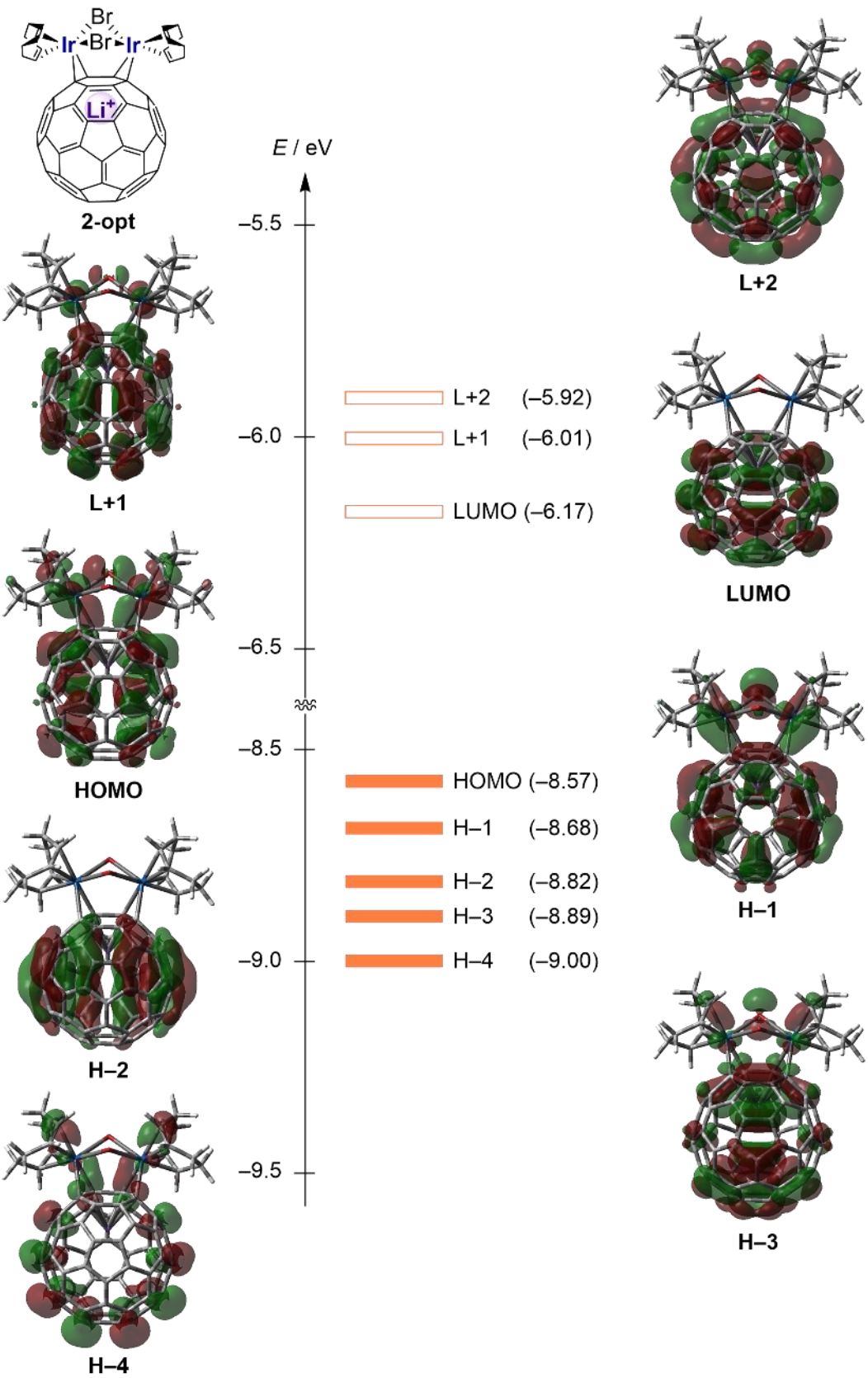

Fig. S27 Kohn-Sham orbitals and energy levels of **2-opt** (from LUMO+2 to HOMO−4, isovalue = 0.02).

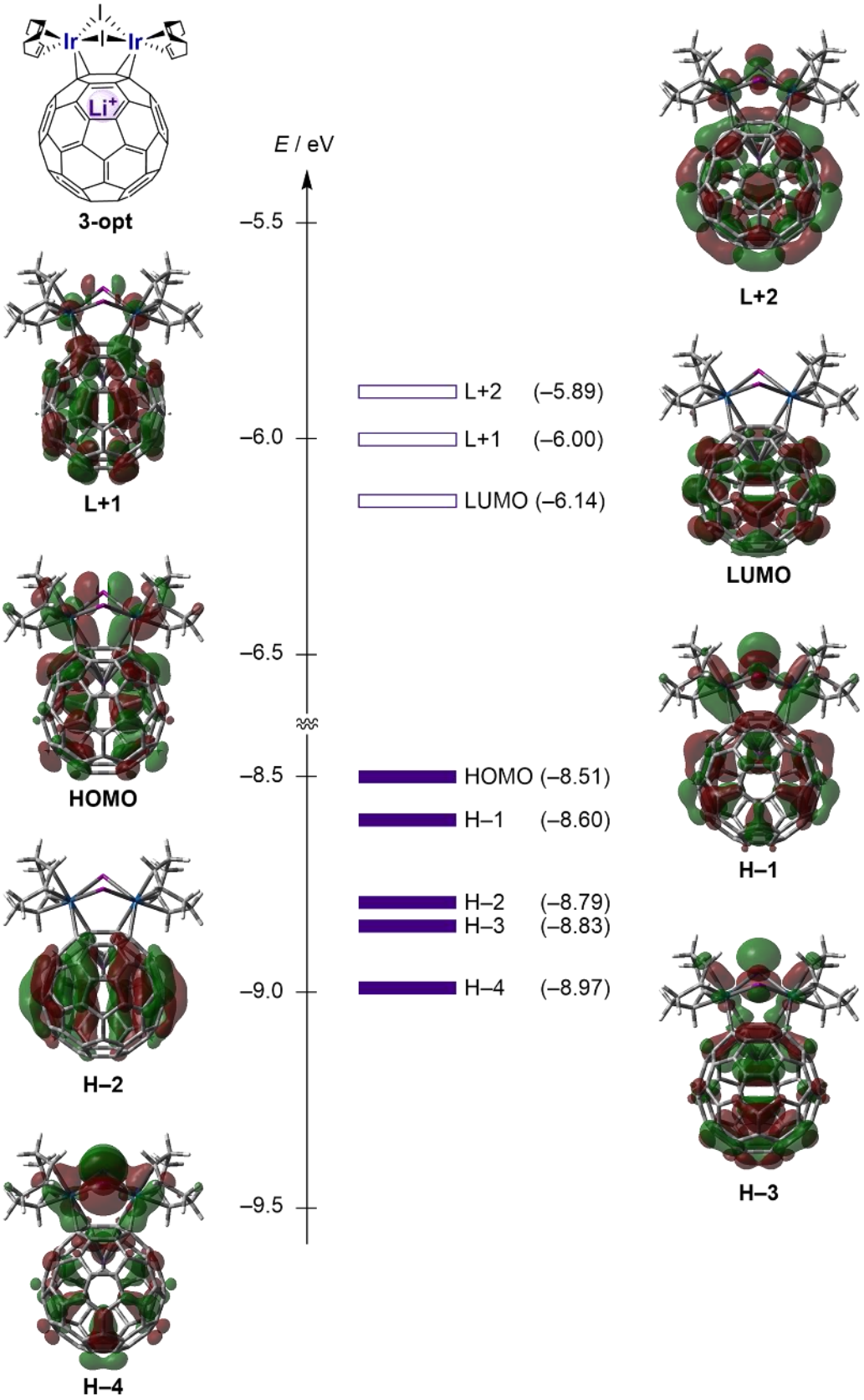

Fig. S28 Kohn-Sham orbitals and energy levels of **3-opt** (from LUMO+2 to HOMO−4, isovalue = 0.02).

6-3. NBO analysis of 1-opt, 2-opt and 3-opt

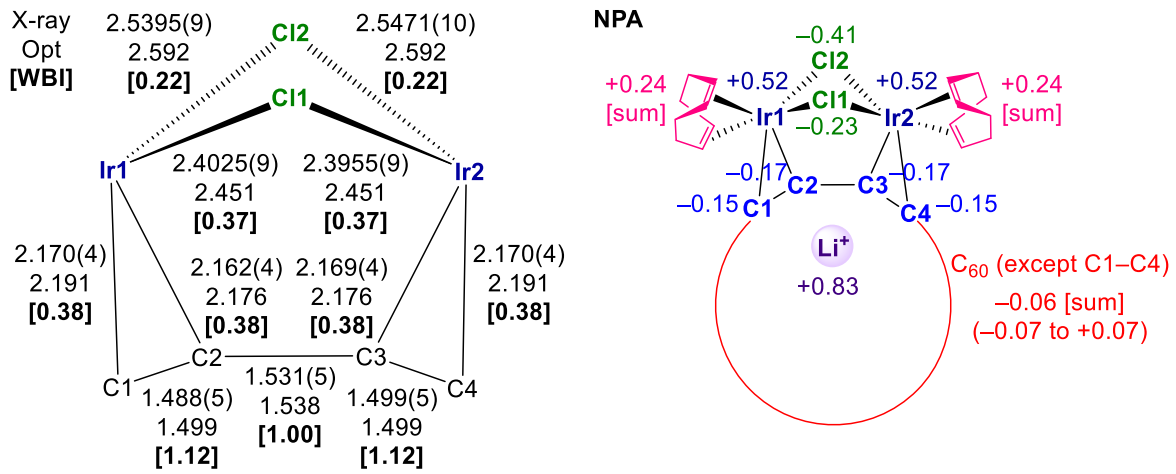

Fig. S29 Selected bond distances (Å), WBI values and NPA charges of **1-opt**.

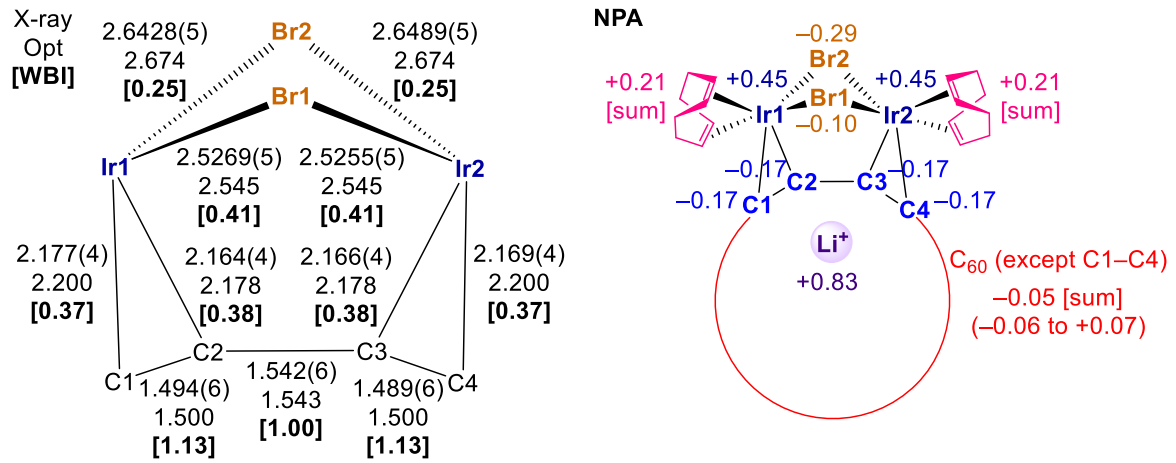

Fig. S30 Selected bond distances (Å), WBI values and NPA charges of **2-opt**.

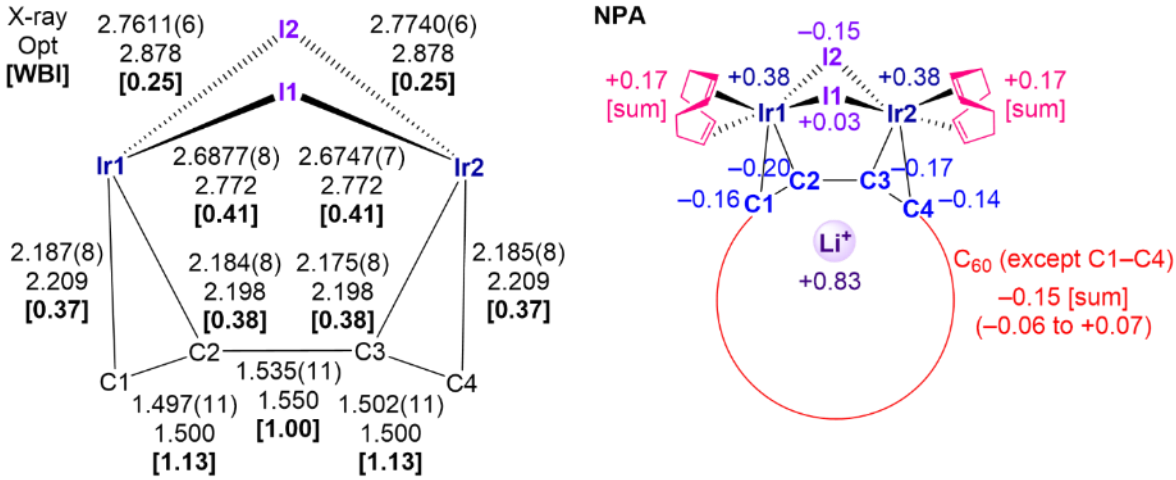

Fig. S31 Selected bond distances (Å), WBI values and NPA charges of **3-opt**.

6-4. GIAO calculations and assignments of the proton signals of cod ligands in 1-opt

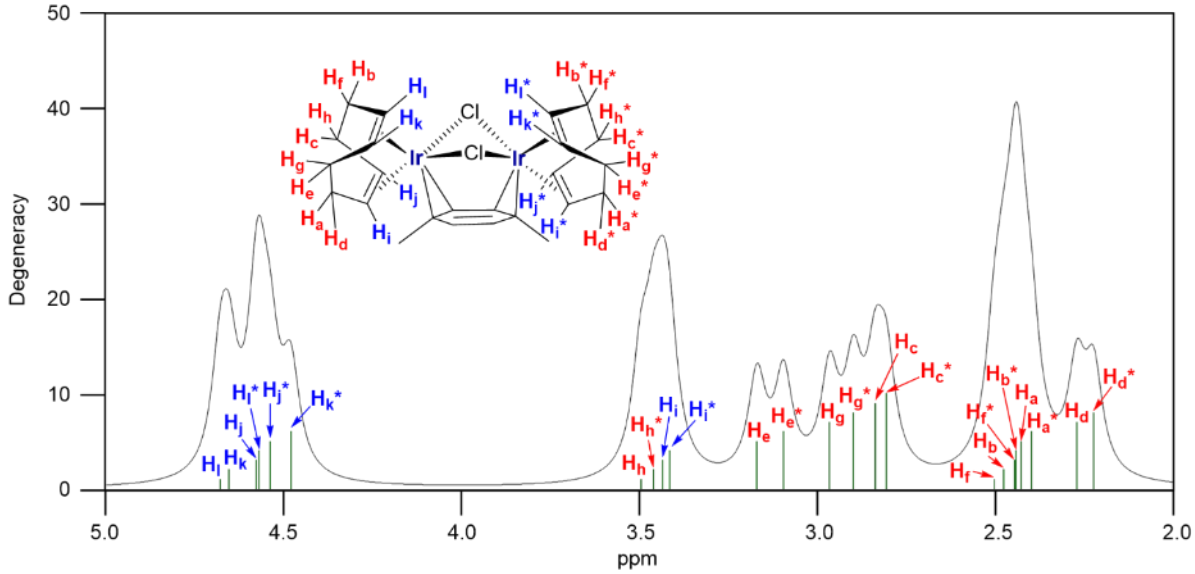

Fig. S32 Simulated ^{1}H NMR spectrum of **1-opt** (degeneracy tolerance: 0.25; peak half-width at half height: 0.03 ppm).

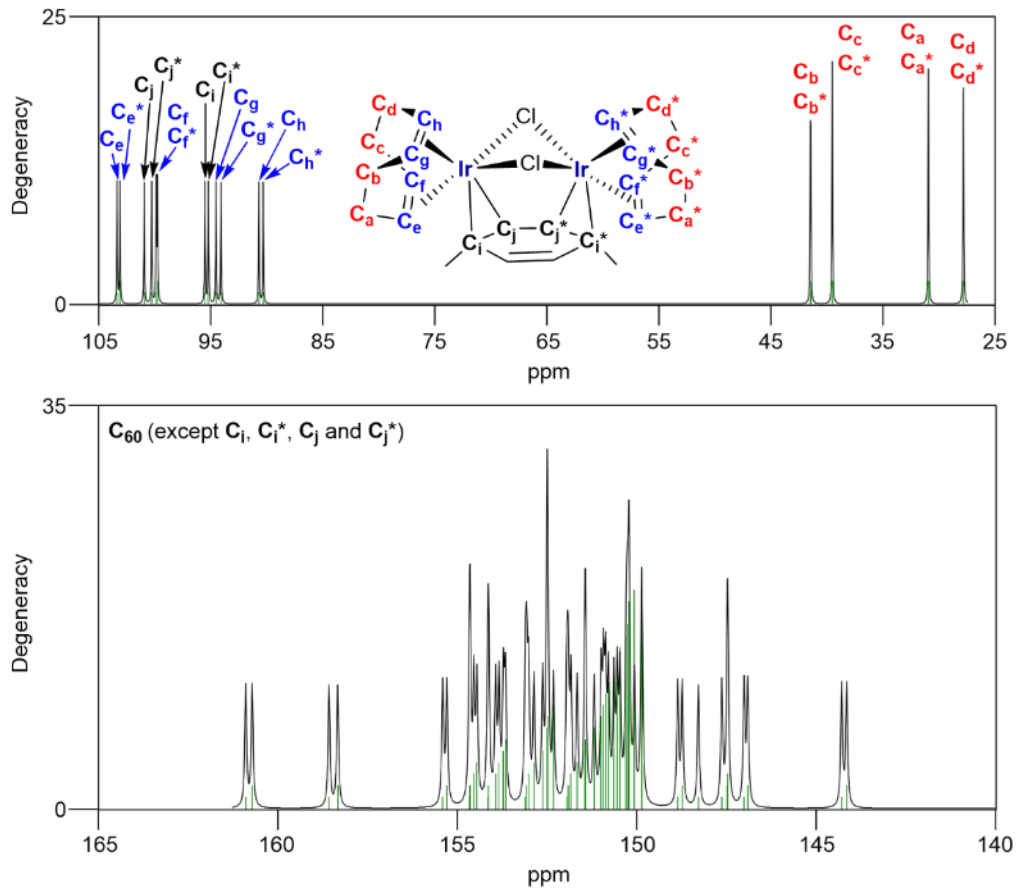

Fig. S33 Simulated ^{13}C NMR spectrum of **1-opt** (degeneracy tolerance: 0.25; peak half-width at half height: 0.03 ppm).

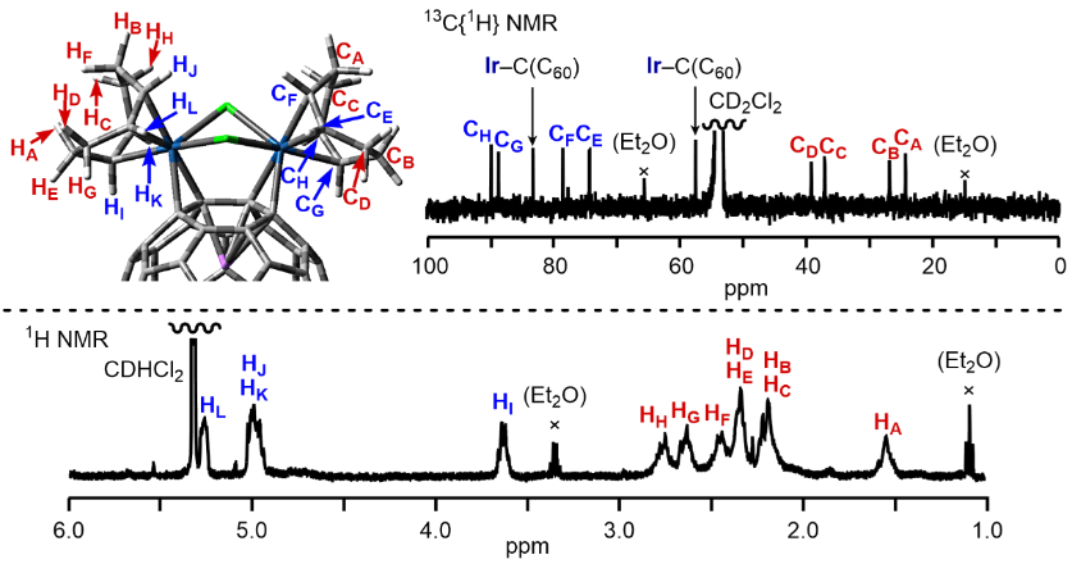

Fig. S34 Assignments of the ^{1}H and ^{13}C NMR signals of the cod ligands of **1** based on 2D NMR spectra (^{1}H–^{1}H COSY and ^{1}H–^{13}C HSQC) and theoretical calculations.

6-5. TD-DFT calculations

Table S10 Excitation energies and oscillator strengths (*f*) of **1** with major optical transitions (threshold: $f \geq 0.01$ except excited state 1).

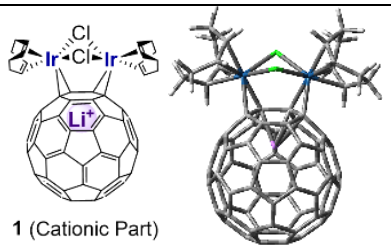

1 (Cationic Part)

Excitation energies and oscillator strengths:

Excited State 1: Singlet-?Sym 1.7985 eV **689.36 nm f=0.0015** <S**2>=0.000
275 -> 276 0.70123 **(98%) H→L**
This state for optimization and/or second-order correction.
Total Energy, E(TD-HF/TD-DFT) = -4046.12527435
Copying the excited state density for this state as the 1-particle RhoCI density.

Excited State 3: Singlet-?Sym 2.0103 eV 616.73 nm f=0.0145 <S**2>=0.000
274 -> 276 -0.27569
274 -> 278 -0.11353
275 -> 277 0.62789

Excited State 10: Singlet-?Sym 2.2920 eV **540.95 nm f=0.0319** <S**2>=0.000
271 -> 277 -0.15114
272 -> 276 -0.12133
272 -> 278 -0.10090
273 -> 277 -0.35567 **(25%) H−2→L+1**
274 -> 278 0.55578 **(62%) H−1→L+2**

Excited State 13: Singlet-?Sym 2.3719 eV 522.72 nm f=0.0103 <S**2>=0.000
271 -> 277 0.34422
272 -> 278 0.57618
273 -> 277 -0.12533
274 -> 278 0.11848

Excited State 21: Singlet-?Sym 2.7778 eV 446.34 nm f=0.0626 <S**2>=0.000
268 -> 278 0.25725
269 -> 277 -0.42209
270 -> 278 0.46926

Excited State 22: Singlet-?Sym 2.7969 eV 443.29 nm f=0.0119 <S**2>=0.000
268 -> 276 0.67764
269 -> 277 -0.11271

Excited State 24: Singlet-?Sym 2.9241 eV **424.01 nm f=0.0821** <S**2>=0.000
265 -> 278 -0.10439
267 -> 277 0.15316
268 -> 278 0.57458 **(66%) H−7→L+2**
268 -> 279 0.10546
270 -> 278 -0.23428 **(11%) H−5→L+2**

Excited State 29: Singlet-?Sym 3.0810 eV 402.42 nm f=0.0153 <S**2>=0.000
267 -> 277 -0.18953
274 -> 279 -0.35861
275 -> 280 0.14595
275 -> 281 0.51210

Excited State 33: Singlet-?Sym 3.1418 eV 394.63 nm f=0.0604 <S**2>=0.000
267 -> 277 -0.39114
269 -> 277 0.10810
274 -> 279 0.44179
275 -> 281 0.10065
275 -> 282 0.23360

Excited State 34: Singlet-?Sym 3.1866 eV 389.08 nm f=0.0381 <S**2>=0.000
262 -> 276 -0.15833
265 -> 278 0.18818
266 -> 277 0.38948
267 -> 277 0.16634
269 -> 280 -0.10797
273 -> 280 0.13294
273 -> 282 -0.13409
274 -> 279 0.17855
275 -> 281 0.23049
275 -> 282 -0.24832

Excited State 39: Singlet-?Sym 3.2287 eV 384.00 nm f=0.0194 <S**2>=0.000
265 -> 278 -0.10500
266 -> 277 0.38912
271 -> 280 0.12413
273 -> 280 0.15107
273 -> 281 0.21432
274 -> 279 -0.10427
275 -> 282 0.44157

Excited State 40: Singlet-?Sym 3.2558 eV 380.81 nm f=0.0119 <S**2>=0.000
264 -> 276 0.11491
265 -> 276 0.19512
265 -> 278 0.39662
265 -> 279 0.11516

267 -> 277 0.20526
273 -> 280 -0.22455
275 -> 282 0.33214

Excited State 44: Singlet-?Sym 3.3037 eV 375.29 nm f=0.0117 <S**2>=0.000
261 -> 277 0.13609
263 -> 276 0.23342
265 -> 278 0.12041
272 -> 279 0.34821
273 -> 280 0.31699
273 -> 281 -0.30870
275 -> 282 0.11590

Excited State 46: Singlet-?Sym 3.3559 eV 369.45 nm f=0.0756 <S**2>=0.000
259 -> 276 0.22524
262 -> 276 0.15573
264 -> 276 -0.24787
264 -> 278 -0.12373
265 -> 276 0.14494
265 -> 278 0.19954
268 -> 278 0.10651
271 -> 280 0.12239
272 -> 279 0.21311
273 -> 281 0.30776
273 -> 282 0.15548
274 -> 279 0.15418
275 -> 282 -0.10299

Excited State 48: Singlet-?Sym 3.3862 eV 366.14 nm f=0.0159 <S**2>=0.000
259 -> 276 -0.22274
260 -> 277 -0.11489
262 -> 276 -0.17209
263 -> 276 -0.18088
263 -> 278 0.20592
270 -> 279 0.10240
271 -> 280 0.35822
271 -> 281 0.17514
272 -> 279 0.22606
273 -> 280 -0.10555
273 -> 282 -0.12290

Excited State 49: Singlet-?Sym 3.4089 eV 363.70 nm f=0.0128 <S**2>=0.000
262 -> 276 0.22735
263 -> 276 0.25237
271 -> 280 0.37678
272 -> 279 -0.29688
273 -> 281 -0.11732
273 -> 282 0.17583

Excited State 55: Singlet-?Sym 3.4938 eV 354.87 nm f=0.0165 <S**2>=0.000
260 -> 277 -0.15057
263 -> 278 -0.12467
264 -> 276 0.44614
271 -> 280 0.18715
271 -> 281 -0.32577
272 -> 279 0.12282
273 -> 281 0.19812
273 -> 282 -0.11024

Excited State 61: Singlet-?Sym 3.5595 eV 348.31 nm f=0.0577 <S**2>=0.000
258 -> 276 -0.15004
258 -> 278 0.15304
259 -> 276 -0.22756
260 -> 277 0.25636
261 -> 277 0.24565
262 -> 278 -0.10260
263 -> 278 0.22907
264 -> 276 0.10092
266 -> 280 -0.10453
268 -> 279 -0.13382
270 -> 279 -0.10727
271 -> 280 -0.10478
273 -> 281 0.20715

Excited State 62: Singlet-?Sym 3.5680 eV 347.49 nm f=0.0150 <S**2>=0.000
257 -> 276 0.19882
259 -> 277 0.38389
263 -> 277 0.11857
268 -> 280 0.14733
269 -> 279 -0.10117
270 -> 280 0.27286
272 -> 280 0.17589
274 -> 281 -0.12446
274 -> 282 0.15176
275 -> 283 -0.21149

Excited State 66: Singlet-?Sym 3.5988 eV 344.52 nm f=0.0174 <S**2>=0.000
260 -> 277 -0.10503
262 -> 278 -0.18870
263 -> 278 0.34909
264 -> 278 -0.29094
265 -> 278 -0.13429
267 -> 280 -0.11781
271 -> 281 -0.25627
271 -> 282 -0.17382
272 -> 279 -0.13601
273 -> 281 -0.12710

Excited State 68: Singlet-?Sym 3.6307 eV 341.49 nm f=0.0116 <S**2>=0.000
258 -> 276 0.36791
260 -> 277 0.32657
261 -> 277 -0.11223
262 -> 276 -0.12566
263 -> 276 0.17823
264 -> 278 0.22915
268 -> 279 -0.13445
270 -> 279 -0.18561
271 -> 280 0.19078

Excited State 69: Singlet-?Sym 3.6437 eV 340.27 nm f=0.0369 <S**2>=0.000
256 -> 276 0.10199
259 -> 276 -0.10751
261 -> 277 -0.34332
262 -> 278 0.37399
263 -> 276 0.15066
263 -> 278 0.21716
271 -> 282 0.24752

Excited State 71: Singlet-?Sym 3.6651 eV 338.29 nm f=0.0161 <S**2>=0.000
257 -> 277 0.10906
258 -> 276 0.47961
261 -> 277 0.12520
264 -> 278 -0.18487
265 -> 278 0.11498
269 -> 280 0.26628
270 -> 279 0.17179
271 -> 280 -0.14016

Excited State 74: Singlet-?Sym 3.6812 eV 336.81 nm f=0.0161 <S**2>=0.000
258 -> 276 0.11384
259 -> 278 0.42374
260 -> 277 -0.21038
261 -> 277 0.15582
262 -> 278 -0.15579
264 -> 278 0.12483
270 -> 279 -0.13089
271 -> 282 0.31863
274 -> 283 0.12248

Excited State 75: Singlet-?Sym 3.7009 eV 335.01 nm f=0.1018 <S**2>=0.000
257 -> 277 0.24296
259 -> 276 -0.12341
259 -> 278 -0.17308
260 -> 277 -0.23824
264 -> 278 0.31043
267 -> 280 -0.14337
269 -> 280 0.20101
271 -> 282 -0.19081
272 -> 279 -0.13782
274 -> 283 0.17053

Excited State 76: Singlet-?Sym 3.7088 eV 334.30 nm f=0.0816 <S**2>=0.000
257 -> 277 -0.24138
258 -> 278 -0.23081
259 -> 278 -0.20375
261 -> 277 0.27746
262 -> 278 0.25439
263 -> 278 0.16198
268 -> 279 0.11900
270 -> 279 -0.23918

Excited State 80: Singlet-?Sym 3.7498 eV **330.64 nm f=0.1094** <S**2>=0.000
256 -> 276 -0.25954 **(13%) H−19→L**
257 -> 277 0.17506
262 -> 278 0.10952
263 -> 278 -0.12129
264 -> 278 -0.12797
265 -> 278 -0.10225
267 -> 280 -0.13995
268 -> 279 -0.22461 **(10%) H−7→L+3**
269 -> 280 0.15357
270 -> 279 -0.10607
271 -> 282 0.28639 **(16%) H−4→L+6**
274 -> 283 -0.24728 **(12%) H−1→L+7**

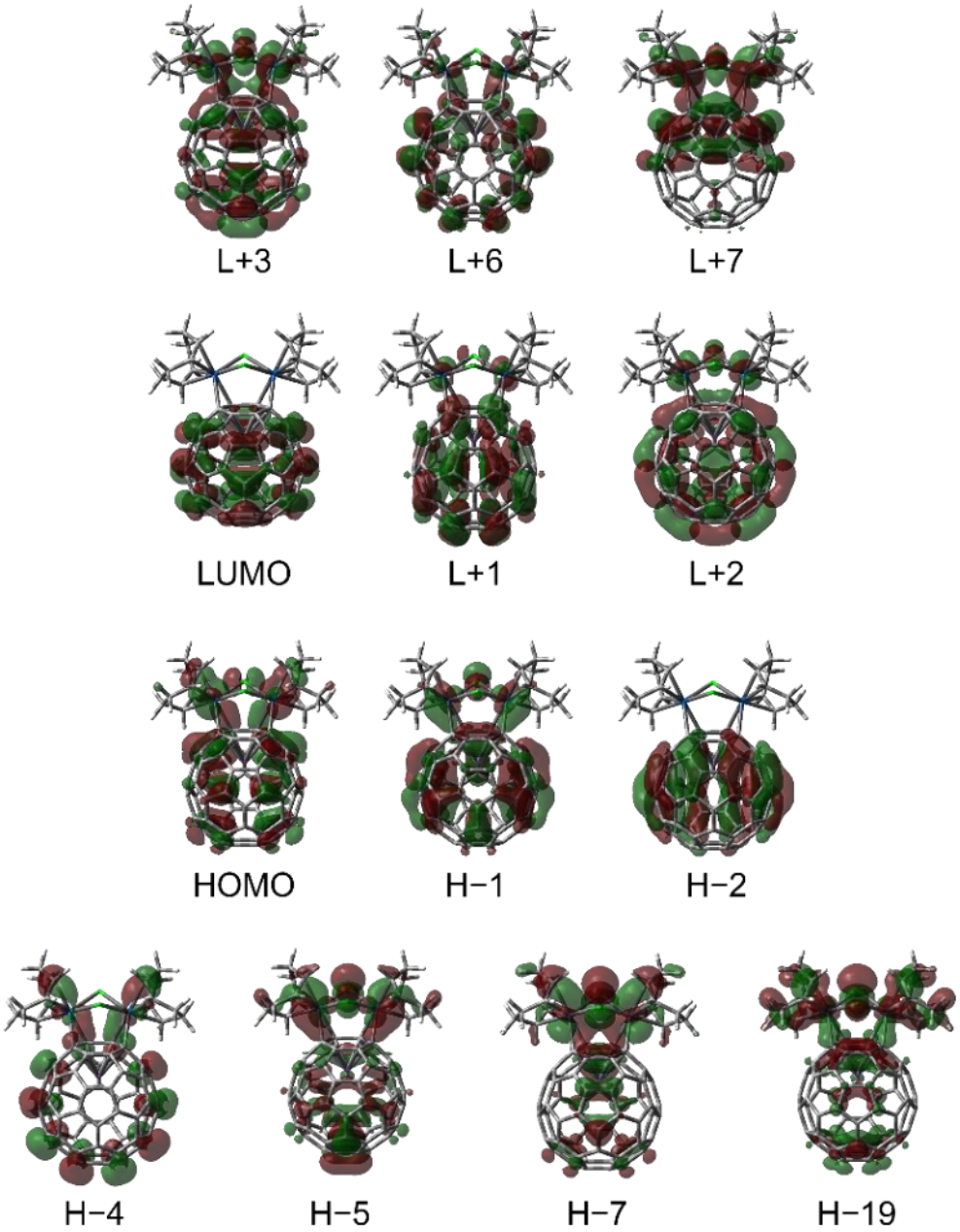

Fig. S35 Kohn-Sham orbitals involved in the main transitions of **1** (isovalue = 0.02).

Table S11 Excitation energies and oscillator strengths (*f*) of **2** with major optical transitions (threshold: $f \geq 0.01$ except excited state 1).

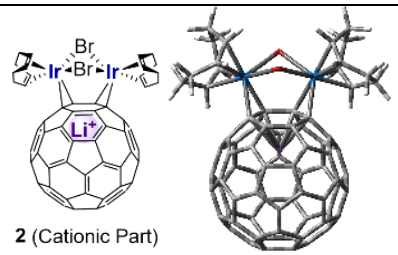

2 (Cationic Part)

Excitation energies and oscillator strengths:

Excited State 1: Singlet-?Sym 1.7872 eV **693.75 nm f=0.0015** <S**2>=0.000
293 -> 294 0.70091 **(98%) H -> L**

This state for optimization and/or second-order correction.
Total Energy, E(TD-HF/TD-DFT) = -8269.31064236
Copying the excited state density for this state as the 1-particle RhoCI density.

Excited State 3: Singlet-?Sym 1.9999 eV 619.96 nm f=0.0146 <S**2>=0.000
292 -> 294 -0.21631
292 -> 296 0.13161
293 -> 295 0.64846

Excited State 8: Singlet-?Sym 2.2671 eV **546.89 nm f=0.0224** <S**2>=0.000
290 -> 294 0.50731 **(51%) H−3→L**
291 -> 295 0.25840 **(13%) H−2→L+1**
292 -> 296 0.39656 **(31%) H−1→L+2**

Excited State 10: Singlet-?Sym 2.2860 eV **542.36 nm f=0.0279** <S**2>=0.000
289 -> 295 -0.14422
291 -> 295 0.50406 **(51%) H−2→L+1**
292 -> 296 -0.44094 **(39%) H−3→L**
293 -> 295 0.11198

Excited State 20: Singlet-?Sym 2.6885 eV 461.16 nm f=0.0236 <S**2>=0.000
286 -> 294 0.64230
286 -> 296 0.11358
288 -> 296 -0.21279

Excited State 21: Singlet-?Sym 2.7140 eV 456.83 nm f=0.0404 <S**2>=0.000
286 -> 294 -0.13210
286 -> 296 0.22974
287 -> 295 0.46801
288 -> 296 -0.42491

Excited State 24: Singlet-?Sym 2.8610 eV **433.36 nm f=0.0843** <S**2>=0.000
285 -> 295 0.10178
286 -> 296 0.60912 **(74%) H−7→L+2**
287 -> 295 -0.13701
288 -> 296 0.20382
293 -> 297 -0.11396

Excited State 25: Singlet-?Sym 2.9195 eV 424.68 nm f=0.0170 <S**2>=0.000
293 -> 297 0.65927
293 -> 299 0.12804

Excited State 32: Singlet-?Sym 3.0805 eV 402.48 nm f=0.0113 <S**2>=0.000
284 -> 294 -0.36827
285 -> 295 0.19681
292 -> 298 0.35609
293 -> 299 0.39137

Excited State 34: Singlet-?Sym 3.1360 eV 395.36 nm f=0.0721 <S**2>=0.000
285 -> 295 0.42867
292 -> 298 -0.41893
293 -> 299 0.10255
293 -> 300 -0.24747

Excited State 36: Singlet-?Sym 3.1725 eV 390.81 nm f=0.0228 <S**2>=0.000
277 -> 294 -0.12020
282 -> 294 -0.10492
283 -> 295 0.11514
284 -> 296 0.40084
284 -> 298 -0.10526
285 -> 295 -0.24985
291 -> 300 -0.12389
292 -> 298 -0.24436
293 -> 299 0.18238
293 -> 300 0.22825

Excited State 38: Singlet-?Sym 3.2037 eV 387.01 nm f=0.0425 <S**2>=0.000
282 -> 294 -0.11352
283 -> 295 0.17849
284 -> 296 -0.33715
285 -> 295 0.19212
290 -> 298 -0.11336
291 -> 299 0.18104
293 -> 300 0.45418

Excited State 42: Singlet-?Sym 3.2656 eV 379.66 nm f=0.0110 <S**2>=0.000
282 -> 294 0.19917
283 -> 295 -0.35088
290 -> 298 0.11109
291 -> 297 0.42007
291 -> 299 -0.16260
293 -> 300 0.25198

Excited State 44: Singlet-?Sym 3.2912 eV 376.71 nm f=0.0232 <S**2>=0.000
279 -> 295 -0.11813
281 -> 294 -0.20977
282 -> 294 -0.29370
290 -> 298 -0.12855
291 -> 297 0.32770
291 -> 299 0.35350
292 -> 298 0.13033
293 -> 300 -0.16993

Excited State 45: Singlet-?Sym 3.3210 eV 373.34 nm f=0.0113 <S**2>=0.000
276 -> 295 -0.10663
278 -> 294 -0.12983
280 -> 295 0.11922
281 -> 295 0.12352
283 -> 296 0.33645
286 -> 297 0.17359
288 -> 297 -0.15432
289 -> 298 0.12770
290 -> 297 0.11972
290 -> 299 0.32938
290 -> 300 0.14258
292 -> 299 0.19126

Excited State 46: Singlet-?Sym 3.3297 eV 372.36 nm f=0.0319 <S**2>=0.000
277 -> 294 -0.28874
281 -> 294 0.23266
282 -> 294 -0.13672
284 -> 296 -0.14630
290 -> 298 0.40290
291 -> 300 -0.21837
292 -> 298 0.13284

Excited State 49: Singlet-?Sym 3.3889 eV 365.85 nm f=0.0138 <S**2>=0.000
277 -> 294 0.23582
278 -> 295 -0.10253
281 -> 296 -0.18569
282 -> 294 -0.12414
288 -> 298 0.12248
289 -> 297 0.42121
289 -> 299 -0.15270
290 -> 298 0.20491
291 -> 297 0.11627

Excited State 53: Singlet-?Sym 3.4337 eV 361.09 nm f=0.0168 <S**2>=0.000
276 -> 294 -0.11333
281 -> 294 0.21561
281 -> 296 0.18582
282 -> 294 -0.29609
282 -> 296 -0.12478
285 -> 297 0.11504
287 -> 297 -0.13324
288 -> 298 0.15318
289 -> 299 0.31981
289 -> 300 0.10139
290 -> 298 -0.13333
291 -> 297 0.10964
291 -> 299 -0.16276

Excited State 55: Singlet-?Sym 3.4622 eV 358.11 nm f=0.0116 <S**2>=0.000
279 -> 294 -0.14247
281 -> 295 0.20779
282 -> 295 -0.20937
283 -> 296 -0.12610
288 -> 297 -0.26343
289 -> 298 0.39813
290 -> 297 -0.21014
290 -> 299 -0.11946
293 -> 301 -0.10567

Excited State 56: Singlet-?Sym 3.4731 eV 356.98 nm f=0.0272 <S**2>=0.000
276 -> 294 -0.10163
278 -> 295 -0.14257
281 -> 294 -0.27464
281 -> 296 0.19120
282 -> 294 0.20862
284 -> 296 -0.10978
285 -> 297 0.12548
287 -> 297 -0.16922
289 -> 299 0.29531
290 -> 298 0.22355
291 -> 299 0.14826

Excited State 58: Singlet-?Sym 3.5013 eV 354.11 nm f=0.0141 <S**2>=0.000
276 -> 294 0.11492
277 -> 294 0.20917
280 -> 294 -0.18582
281 -> 296 0.10294
282 -> 294 -0.11958
282 -> 296 0.30051
283 -> 295 -0.10588
284 -> 296 -0.12543
285 -> 297 0.10245
287 -> 297 -0.18764
288 -> 298 -0.11242
289 -> 297 -0.17559
289 -> 299 -0.17714
291 -> 299 -0.17520
291 -> 300 -0.16307

Excited State 63: Singlet-?Sym 3.5494 eV 349.31 nm f=0.0415 <S**2>=0.000
277 -> 294 0.22759
278 -> 295 0.24349
279 -> 295 0.14911
280 -> 296 -0.14205
281 -> 296 -0.18537
282 -> 296 -0.18999
286 -> 298 0.20635
288 -> 298 -0.17548
289 -> 299 0.13740
291 -> 299 0.17821
291 -> 300 -0.20370

Excited State 66: Singlet-?Sym 3.5821 eV 346.12 nm f=0.0383 <S**2>=0.000
276 -> 294 -0.14728
279 -> 295 0.27313
280 -> 294 -0.18539
281 -> 296 0.11272
288 -> 298 0.33320
289 -> 297 -0.15628
289 -> 299 -0.21557
291 -> 299 0.22654

Excited State 70: Singlet-?Sym 3.6165 eV 342.82 nm f=0.0102 <S**2>=0.000
275 -> 295 -0.11317
276 -> 294 -0.24505
277 -> 294 0.11901
279 -> 295 -0.16598
280 -> 294 -0.15898
280 -> 296 0.11338
281 -> 296 0.33241
282 -> 296 -0.18633
287 -> 297 0.18846
288 -> 298 -0.23741
289 -> 297 0.18456
289 -> 300 0.12662
292 -> 301 -0.10761

Excited State 71: Singlet-?Sym 3.6352 eV 341.07 nm f=0.0747 <S**2>=0.000
275 -> 295 0.12227
276 -> 294 0.12824
277 -> 296 0.15779
279 -> 295 -0.27845
280 -> 296 0.35044
281 -> 296 -0.12490
282 -> 296 -0.16878
287 -> 297 -0.23038
289 -> 300 0.17493
291 -> 299 0.10014

Excited State 75: Singlet-?Sym 3.6733 eV 337.53 nm f=0.0171 <S**2>=0.000
274 -> 294 -0.20189

276 -> 296 -0.22139
278 -> 295 0.31198
279 -> 295 -0.24375
280 -> 296 0.11981
286 -> 298 0.17338
288 -> 298 0.16292
289 -> 300 -0.24993
292 -> 301 0.17377

Excited State 76: Singlet-?Sym 3.6923 eV 335.79 nm f=0.0436 <S**2>=0.000
275 -> 295 0.31089
276 -> 296 0.14839
278 -> 295 -0.21001
280 -> 296 -0.26682
281 -> 296 0.26888
285 -> 297 -0.16638
286 -> 298 0.21051
288 -> 298 0.10073

Excited State 79: Singlet-?Sym 3.7186 eV 333.42 nm f=0.0191 <S**2>=0.000
274 -> 295 -0.13612
275 -> 296 0.31643
279 -> 296 -0.19364
280 -> 295 -0.11156
281 -> 295 0.12114
284 -> 297 -0.17268
285 -> 298 0.12072
286 -> 297 0.10610
287 -> 298 0.36882
288 -> 300 0.15733
290 -> 300 -0.14387
293 -> 301 -0.13851

Excited State 80: Singlet-?Sym 3.7207 eV **333.23 nm f=0.1083** <S**2>=0.000
276 -> 294 -0.16989
276 -> 296 0.37217 **(28%) H−17→L+2**
277 -> 296 0.13035
278 -> 295 0.15265
280 -> 296 0.15365
282 -> 296 0.18536
286 -> 298 0.14235
287 -> 297 -0.15686
289 -> 300 0.25193 **(13%) H−4→L+6**
292 -> 301 0.24837 **(12%) H−1→L+7**

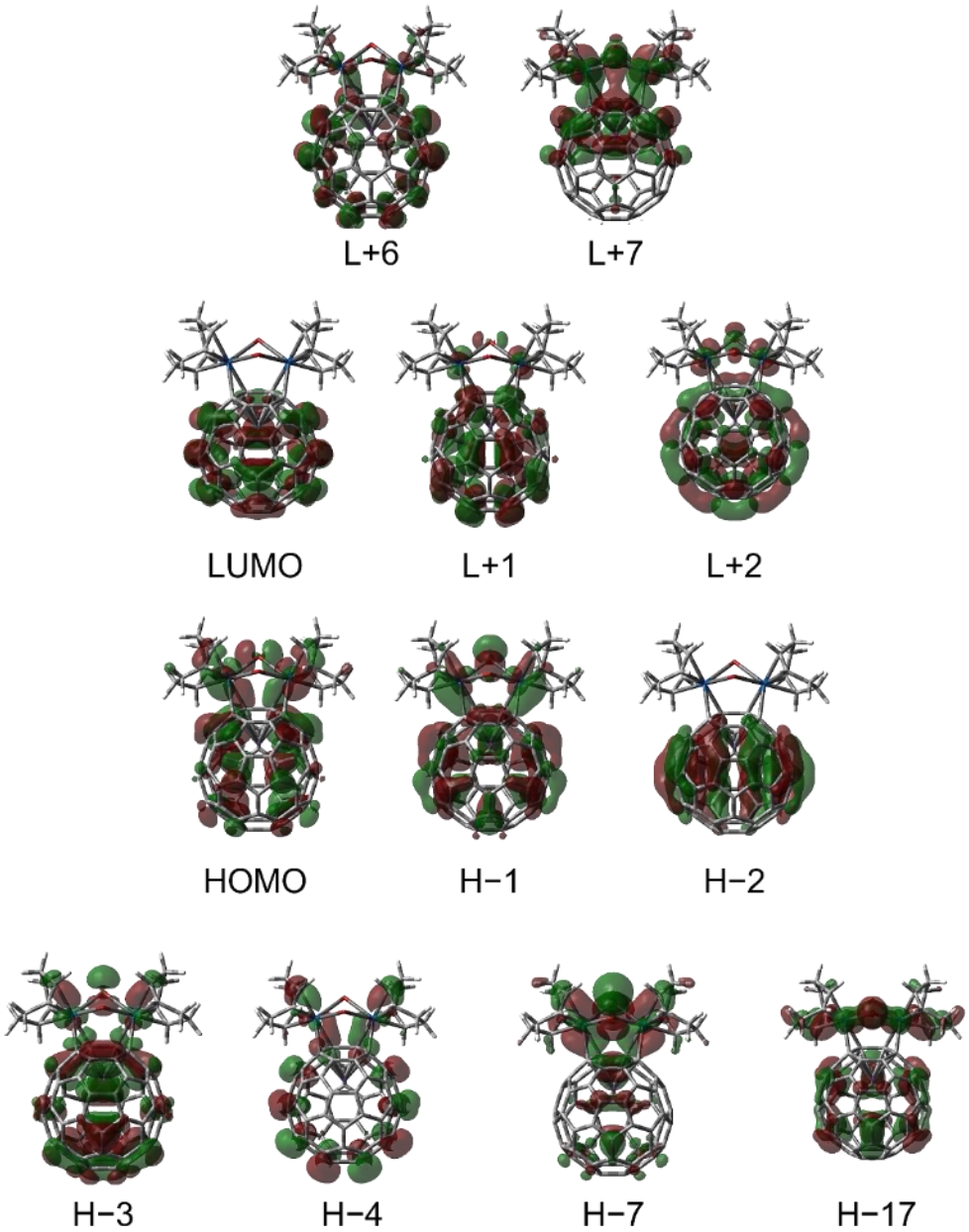

Fig. S36 Kohn-Sham orbitals involved in the main transitions of **2** (isovalue = 0.02).

Table S12 Excitation energies and oscillator strengths (*f*) of **3** with major optical transitions (threshold: $f \geq 0.01$ except excited state 1).

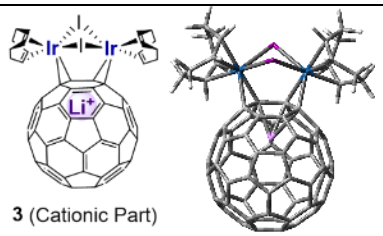

3 (Cationic Part)

Excitation energies and oscillator strengths:

Excited State 1: Singlet-?Sym 1.7585 eV **705.05 nm f=0.0015** <S**2>=0.000
283 -> 284 0.69940 **(98%) H→L**
This state for optimization and/or second-order correction.
Total Energy, E(TD-HF/TD-DFT) = -3721.52770114
Copying the excited state density for this state as the 1-particle RhoCI density.

Excited State 3: Singlet-?Sym 1.9559 eV 633.90 nm f=0.0157 <S**2>=0.000
282 -> 284 0.21141
282 -> 286 -0.14499
283 -> 285 0.64808

Excited State 7: Singlet-?Sym 2.1389 eV 579.67 nm f=0.0168 <S**2>=0.000
280 -> 284 0.46719
281 -> 285 -0.35241
282 -> 286 0.34998
283 -> 285 0.10051

Excited State 8: Singlet-?Sym 2.2313 eV **555.66 nm f=0.0520** <S**2>=0.000
280 -> 284 -0.45666 **(42%) H−3→L**
282 -> 286 0.50355 **(51%) H−1→L+2**

Excited State 10: Singlet-?Sym 2.2620 eV 548.11 nm f=0.0190 <S**2>=0.000
278 -> 285 -0.10283
279 -> 284 0.15444
280 -> 284 0.20085
281 -> 285 0.56674
282 -> 286 0.29043
283 -> 285 0.10044

Excited State 22: Singlet-?Sym 2.6032 eV 476.27 nm f=0.0429 <S**2>=0.000
276 -> 286 -0.19807
277 -> 285 0.52740
278 -> 285 0.10511
279 -> 286 -0.37229

Excited State 25: Singlet-?Sym 2.6927 eV 460.44 nm f=0.0101 <S**2>=0.000
277 -> 286 -0.23749
279 -> 285 0.17235
279 -> 287 -0.11353
280 -> 287 -0.11118
282 -> 287 0.58948

Excited State 26: Singlet-?Sym 2.6982 eV 459.50 nm f=0.0524 <S**2>=0.000
276 -> 286 0.55383
279 -> 286 -0.21803
283 -> 287 0.29728

Excited State 30: Singlet-?Sym 2.9024 eV **427.17 nm f=0.0151** <S**2>=0.000
274 -> 285 0.24604 **(12%) H−9→L+1**
275 -> 286 0.58844 **(69%) H−3→L+2**
279 -> 288 -0.11578

Excited State 33: Singlet-?Sym 3.0235 eV 410.07 nm f=0.0297 <S**2>=0.000
274 -> 285 0.46601
274 -> 287 0.10542
275 -> 286 -0.27627
282 -> 288 -0.35558
283 -> 289 0.15560

Excited State 35: Singlet-?Sym 3.0313 eV 409.01 nm f=0.0582 <S**2>=0.000
274 -> 285 0.29718
274 -> 287 0.12220
275 -> 286 -0.13981
277 -> 287 -0.12358
282 -> 288 0.42712
283 -> 289 -0.36446

Excited State 36: Singlet-?Sym 3.0586 eV 405.37 nm f=0.0548 <S**2>=0.000
273 -> 285 -0.16526
274 -> 285 0.11526
282 -> 288 0.33592
283 -> 289 0.48896
283 -> 290 0.21667

Excited State 40: Singlet-?Sym 3.1265 eV 396.56 nm f=0.0540 <S**2>=0.000
271 -> 284 0.13160
272 -> 284 0.11806
273 -> 285 -0.16683
274 -> 285 0.11138
277 -> 287 0.26929
281 -> 289 -0.11592
282 -> 288 -0.12442
283 -> 289 -0.21605
283 -> 290 0.46648

Excited State 45: Singlet-?Sym 3.2197 eV 385.08 nm f=0.0306 <S**2>=0.000
272 -> 284 0.20706
273 -> 285 0.28950
274 -> 285 -0.21691
274 -> 287 0.15891
277 -> 287 -0.26773
278 -> 287 -0.15346
281 -> 289 -0.17184
283 -> 290 0.30499

Excited State 49: Singlet-?Sym 3.2823 eV 377.74 nm f=0.0118 <S**2>=0.000
267 -> 284 0.15053
273 -> 286 0.49022
278 -> 288 0.19588
280 -> 287 -0.14908
280 -> 289 0.12392
281 -> 288 -0.21731
282 -> 289 -0.18562
283 -> 291 0.14306

Excited State 50: Singlet-?Sym 3.3132 eV 374.21 nm f=0.0645 <S**2>=0.000
271 -> 286 -0.14567
272 -> 284 0.10241
272 -> 286 0.26056
273 -> 285 -0.32001
275 -> 288 0.10282
277 -> 287 -0.20756
278 -> 287 0.34749
280 -> 288 -0.11762
282 -> 291 -0.10270

Excited State 55: Singlet-?Sym 3.3695 eV 367.96 nm f=0.0140 <S**2>=0.000
268 -> 285 0.10589
269 -> 284 -0.14774
271 -> 285 -0.11550
272 -> 285 -0.25563
274 -> 286 0.15317
276 -> 287 -0.15071
277 -> 288 0.22099
278 -> 288 0.29628
280 -> 289 -0.16248
280 -> 290 0.13155
282 -> 290 -0.13350
283 -> 291 0.26714

Excited State 56: Singlet-?Sym 3.3737 eV 367.51 nm f=0.0276 <S**2>=0.000
271 -> 284 0.23446
272 -> 284 0.27623
272 -> 286 0.10505
276 -> 288 0.17476
278 -> 289 -0.12481
279 -> 288 0.29732
281 -> 289 0.28483
282 -> 291 -0.11084

Excited State 61: Singlet-?Sym 3.4488 eV 359.50 nm f=0.0131 <S**2>=0.000
266 -> 284 0.15024
268 -> 284 -0.23906
270 -> 284 0.20732
271 -> 286 -0.25841
272 -> 286 -0.13129
278 -> 289 0.42558
281 -> 289 0.14401
281 -> 290 -0.14969

Excited State 64: Singlet-?Sym 3.4778 eV 356.50 nm f=0.0854 <S**2>=0.000
266 -> 284 -0.27543
269 -> 285 -0.12702
271 -> 286 -0.16394
272 -> 284 -0.14176
272 -> 286 0.18491
276 -> 288 -0.14199
277 -> 287 0.13089
279 -> 288 0.37920
281 -> 289 -0.26389

Excited State 69: Singlet-?Sym 3.5213 eV 352.09 nm f=0.0157 <S**2>=0.000
266 -> 284 -0.30684
268 -> 284 -0.24275
269 -> 285 0.11014
276 -> 288 0.14182
278 -> 289 0.13143
281 -> 289 0.11677
281 -> 290 0.49517

Excited State 72: Singlet-?Sym 3.5632 eV 347.96 nm f=0.0368 <S**2>=0.000
266 -> 284 0.19168
267 -> 285 -0.10389
268 -> 284 -0.21477
269 -> 285 -0.21744
270 -> 286 -0.10625
272 -> 286 0.30288
274 -> 287 -0.18977
276 -> 288 0.21666
278 -> 290 0.10927
281 -> 289 -0.22347

282 -> 291 0.17219

Excited State 78: Singlet-?Sym 3.6132 eV 343.14 nm f=0.0124 <S**2>=0.000
267 -> 285 -0.16213
268 -> 286 -0.21803
270 -> 286 0.35445
278 -> 290 -0.17844
279 -> 288 0.14178
282 -> 291 0.40461

Excited State 79: Singlet-?Sym 3.6319 eV 341.38 nm f=0.0308 <S**2>=0.000
264 -> 285 -0.13275
265 -> 284 -0.19333
265 -> 286 -0.19013
266 -> 285 -0.25223
267 -> 286 0.35378
268 -> 285 0.10305
269 -> 284 0.14349
277 -> 288 -0.11076
279 -> 289 -0.27451
279 -> 290 0.15526

Excited State 80: Singlet-?Sym 3.6348 eV **341.11 nm f=0.0813** <S**2>=0.000
265 -> 285 0.26701 **(14%) H−18→L+1**
267 -> 285 0.10136
268 -> 284 -0.12069
268 -> 286 0.24564 **(12%) H−15→L+2**
269 -> 285 0.11535
270 -> 286 0.33148 **(22%) H−13→L+2**
271 -> 286 0.21941
274 -> 287 0.12216
275 -> 288 0.16768
276 -> 288 0.11704
277 -> 290 -0.11886
278 -> 290 0.10298
281 -> 289 -0.11030

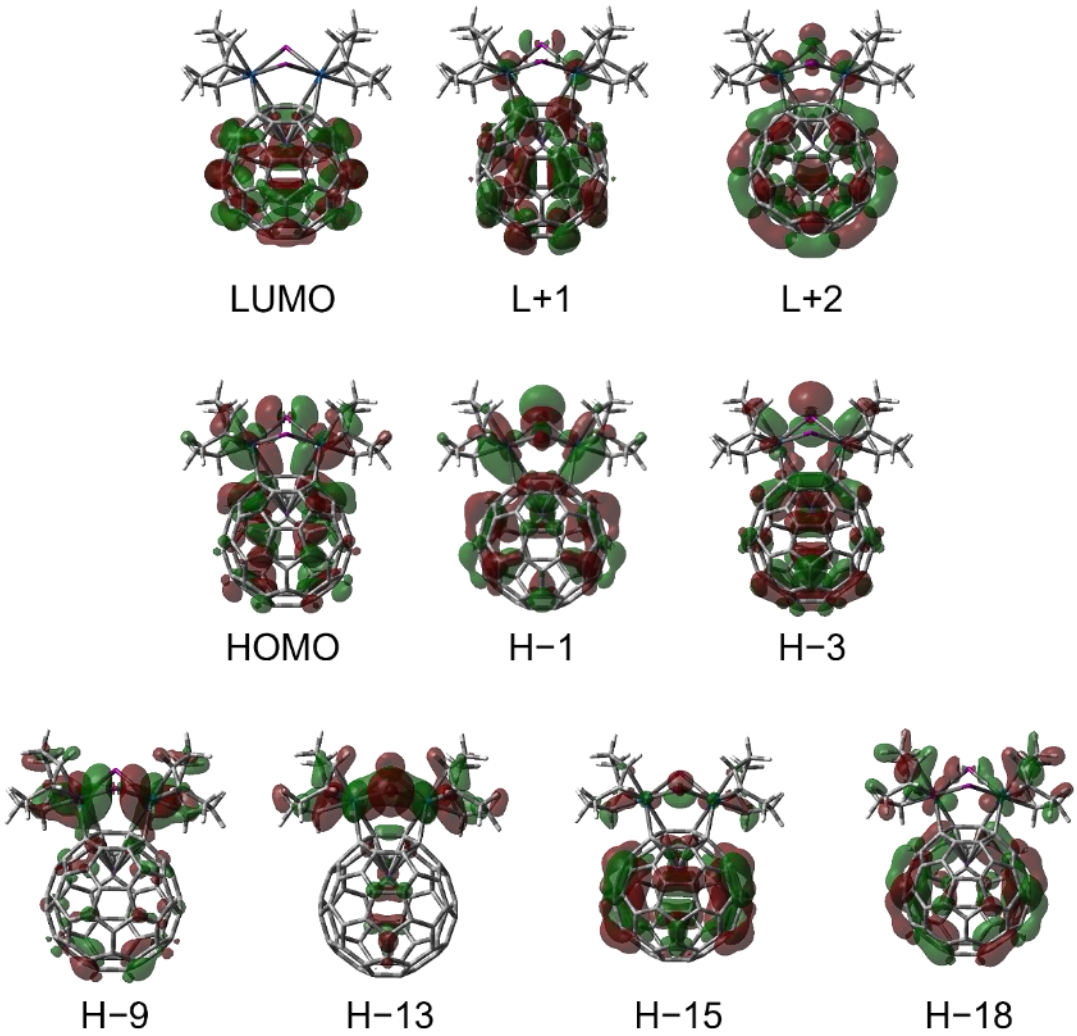

Fig. S37 Kohn-Sham orbitals involved in the main transitions of **3** (isovalue = 0.02).

7. References

[S1] L. Jürgensen, M. Frank, M. Pyeon, L. Czympiel and S. Mathur, *Organometallics*, 2017, **36**, 2331–2337.

[S2] T. Yamagata, H. Tadaoka, M. Nagata, T. Hirao, Y. Kataoka, V. Ratovelomanana-Vidal, J. P. Genet and K. Mashima, *Organometallics*, 2006, **25**, 2505–2513.

[S3] H. Okada and Y. Matsuo, *Fuller. Nanotub. Car. N.*, 2014, **22**, 262–268.

[S4] G. M. Sheldrick, *Acta Cryst.*, 2015, **A71**, 3–8.

[S5] G. M. Sheldrick, *Acta Cryst.*, 2015, **C71**, 3–8.

[S6] O. V. Dolomanov, L. J. Bourhis, R. J. Gildea, J. A. K. Howard and H. Puschmann, *J. Appl. Cryst.*, 2009, **42**, 339–341.

[S7] K. Wakita, *Yadokari-XG*, *Software for Crystal Structure Analyses*, 2001.

[S8] C. Kabuto, S. Akine, T. Nemoto and E. Kwon, *J. Cryst. Soc. Jpn.*, 2009, **51**, 218–224.

[S9] H. Okada, T. Komuro, T. Sakai, Y. Matsuo, Y. Ono, K. Omote, K. Yokoo, K. Kawachi, Y. Kasama, S. Ono, R. Hatakeyama, T. Kaneko and H. Tobita, *RSC Adv.* 2012, **2**, 10624–10631.

[S10] M. J. Frisch, G. W. Trucks, H. B. Schlegel, G. E. Scuseria, M. A. Robb, J. R. Cheeseman, G. Scalmani, V. Barone, G. A. Petersson, H. Nakatsuji, X. Li, M. Caricato, A. V. Marenich, J. Bloino, B. G. Janesko, R. Gomperts, B. Mennucci, H. P. Hratchian, J. V. Ortiz, A. F. Izmaylov, J. L. Sonnenberg, D. W.-Young, F. Ding, F. Lipparini, F. Egidi, J. Goings, B. Peng, A. Petrone, T. Henderson, D. Ranasinghe, V. G. Zakrzewski, J. Gao, N. Rega, G. Zheng, W. Liang, M. Hada, M. Ehara, K. Toyota, R. Fukuda, J. Hasegawa, M. Ishida, T. Nakajima, Y. Honda, O. Kitao, H. Nakai, T. Vreven, K. Throssell, J. A. Montgomery, Jr., J. E. Peralta, F. Ogliaro, M. J. Bearpark, J. J. Heyd, E. N. Brothers, K. N. Kudin, V. N. Staroverov, T. A. Keith, R. Kobayashi, J. Normand, K. Raghavachari, A. P. Rendell, J. C. Burant, S. S. Iyengar, J. Tomasi, M. Cossi, J. M. Millam, M. Klene, C. Adamo, R. Cammi, J. W. Ochterski, R. L. Martin, K. Morokuma, O. Farkas, J. B. Foresman and D. J. Fox, *Gaussian 16*, *(Revision C.02)*, Gaussian, Inc., Wallingford CT, 2019.

[S11] A. D. Becke, *J. Chem. Phys.*, 1993, **98**, 5648–5652.

[S12] J. P. Perdew, *Electronic Structure of Solids '91*, ed. P. Ziesche and H. Eschrig, Akademie Verlag, Berlin, 1991, p. 11.

[S13] J. P. Perdew, K. Burke and Y. Wang, *Phys. Rev. B*, 1996, **54**, 16533–16539.

[S14] W. J. Hehre, R. Ditchfield and J. A. Pople, *J. Chem. Phys.*, 1972, **56**, 2257–2261.

[S15] P. C. Hariharan and J. A. Pople, *Theor. Chim. Acta*, 1973, **28**, 213–222.

[S16] M. M. Francl, W. J. Pietro, W. J. Hehre, J. S. Binkley, M. S. Gordon, D. J. DeFrees and J. A. Pople, *J. Chem. Phys.*, 1982, **77**, 3654–3665.

[S17] P. J. Hay and W. R. Wadt, *J. Chem. Phys.*, 1985, **82**, 299–310.

[S18] K. B. Wiberg, *Tetrahedron*, 1968, **24**, 1083–1096.

[S19] A. E. Reed, R. B. Weinstock and F. Weinhold, *J. Chem. Phys.*, 1985, **83**, 735–746.

[S20] E. D. Glendening, J, K. Badenhoop, A. E. Reed, J. E. Carpenter, J. A. Bohmann, C. M. Morales, P. Karafiloglou, C. R. Landis and F. Weinhold, *NBO 7.0*, Theoretical Chemistry Institute, University of Wisconsin, Madison, 2018.

[S21] T. Clark, J. Chandrasekhar, G. W. Spitznagel and P. von R. Schleyer, *J. Comp. Chem.*, 1983, **4**, 294–301.

[S22] W. T. Chan and R. Fournier, *Chem. Phys. Lett.*, 1999, **315**, 257–265.

[S23] S. Grimme, J. Antony, S. Ehrlich and H. Krieg, *J. Chem. Phys.*, 2010, **132**, 154104.

[S24] K. Wolinski, J. F. Hinton and P. Pulay, *J. Am. Chem. Soc.*, 1990, **112**, 8251–8260.

[S25] F. Weigend and R. Ahlrichs, *Phys. Chem. Chem. Phys.*, 2005, **7**, 3297–3305.

[S26] F. Weigend, *Phys. Chem. Chem. Phys.*, 2006, **8**, 1057–1065.

[S27] A. V. Marenich, C. J. Cramer and D. G. Truhlar, *J. Phys. Chem. B*, 2009, **113**, 6378–6396.